NEURAL REGENERATION RESEARCH
www.nrronline.org

Research Article

Changes in border-associated macrophages after stroke: Single-cell sequencing analysis

Ning Yu, Yang Zhao, Peng Wang, Fuqiang Zhang, Cuili Wen, Shilei Wang*

https://doi.org/10.4103/NRR.NRR-D-24-01092
Date of submission: September 17, 2024
Date of decision: December 9, 2024
Date of acceptance: December 27, 2024
Date of web publication: January 29, 2025

From the Contents

Introduction
Methods
Results
Discussion

Graphical Abstract

Comprehensive changes in border-associated macrophages (BAMs) after stroke

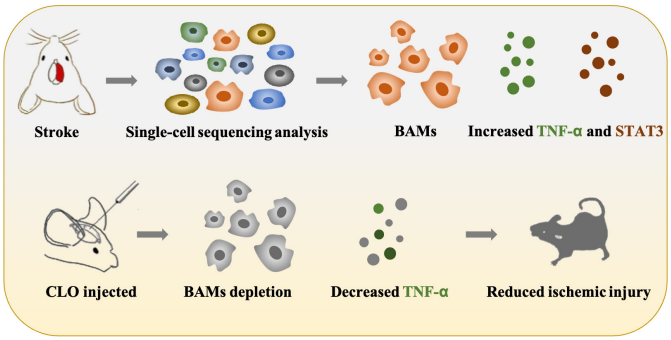

Abstract

Border-associated macrophages are located at the interface between the brain and the periphery, including the perivascular spaces, choroid plexus, and meninges. Until recently, the functions of border-associated macrophages have been poorly understood and largely overlooked. However, a recent study reported that border-associated macrophages participate in stroke-induced inflammation, although many details and the underlying mechanisms remain unclear. In this study, we performed a comprehensive single-cell analysis of mouse border-associated macrophages using sequencing data obtained from the Gene Expression Omnibus (GEO) database (GSE174574 and GSE225948). Differentially expressed genes were identified, and enrichment analysis was performed to identify the transcription profile of border-associated macrophages. CellChat analysis was conducted to determine the cell communication network of border-associated macrophages. Transcription factors were predicted using the 'pySCENIC' tool. We found that, in response to hypoxia, border-associated macrophages underwent dynamic transcriptional changes and participated in the regulation of inflammatory-related pathways. Notably, the tumor necrosis factor pathway was activated by border-associated macrophages following ischemic stroke. The pySCENIC analysis indicated that the activity of signal transducer and activator of transcription 3 (Stat3) was obviously upregulated in stroke, suggesting that Stat3 inhibition may be a promising strategy for treating border-associated macrophages-induced neuroinflammation. Finally, we constructed an animal model to investigate the effects of border-associated macrophages depletion following a stroke. Treatment with liposomes containing clodronate significantly reduced infarct volume in the animals and improved neurological scores compared with untreated animals. Taken together, our results demonstrate comprehensive changes in border-associated macrophages following a stroke, providing a theoretical basis for targeting border-associated macrophages-induced neuroinflammation in stroke treatment.

Key Words: border-associated macrophages; clodronate; hypoxia; ischemia-reperfusion; ischemic stroke; liposomes; neuroinflammation; single-cell sequencing analysis; STAT3; tumor necrosis factor

Introduction

Ischemic stroke is characterized by a high mortality rate (Feigin et al., 2022), and its incidence and prevalence are rapidly increasing worldwide. Due to a lack of early predictive indicators and effective therapeutic strategies, many patients who experience a stroke are left with lasting disabilities (Paul and Candelario-Jalil, 2021). Therefore, there is an urgent need for novel treatment strategies for patients experiencing acute ischemic stroke.

After ischemic stroke, reperfusion-induced inflammatory injury continues to exacerbate cerebral tissue damage and expand the extent of lesions (DeLong et al., 2022; Cai et al., 2023). Accumulating evidence suggests that carefully monitoring inflammation could create a conducive environment for tissue restoration, ultimately improving patient outcomes (Cai et al., 2019, 2023). Brain-resident macrophages (microglia) are the first responders following ischemic stroke (Tan et al., 2024). Then, numerous monocytes from the peripheral blood infiltrate the injured region and induce a series of inflammatory responses (Gelderblom et al., 2009; Wicks et al., 2022; Wang et al., 2025). Blocking macrophage-induced neuroinflammation, which regulates tissue repair and regeneration in the ischemic microenvironment, is a promising therapeutic objective in ischemic stroke.

Tissue-resident macrophages are crucial for maintaining local homeostasis and conducting immune surveillance. The central nervous system is immune-privileged, primarily because the blood–brain barrier restricts the entry of microorganisms and the influx of circulating immune cells. Within the central nervous system, brain macrophages are anatomically categorized into parenchymal microglia and non-parenchymal border-associated macrophages (BAMs). BAMs were discovered significantly later than microglia, but research on BAMs has evolved rapidly, driven by innovative technologies including mass spectrometry cell analysis, fate mapping, single-cell RNA sequencing, *in vivo* imaging, and Cre recombinase-mediated mutagenesis. Moreover, BAMs are thought to play a crucial role in regulating neuroimmune responses related to the brain's barriers and may contribute to immune-mediated neuropathological conditions. Importantly, BAMs have been identified as active participants in various cerebral pathologies, such as ischemic stroke,

Department of Anesthesiology, Shandong Provincial Key Medical and Health Laboratory of Anesthesia and Brain Function (The Affiliated Hospital of Qingdao University), The Affiliated Hospital of Qingdao University, Qingdao, Shandong Province, China
*Correspondence to: Shilei Wang, MD, wshlei@aliyun.com.
https://orcid.org/0000-0002-5762-539X (Shilei Wang)

Funding: This study was supported by Qingdao Key Medical and Health Discipline Project; The Intramural Research Program of the Affiliated Hospital of Qingdao University, No. 4910; and Qingdao West Coast New Area Science and Technology Project, No. 2020-55 (all to SW).
How to cite this article: Yu N, Zhao Y, Wang P, Zhang F, Wen C, Wang S (2026) Changes in border-associated macrophages after stroke: Single-cell sequencing analysis. Neural Regen Res 21(1):346-356.

Parkinson's disease, Alzheimer's disease, and gliomas. BAMs were found in leptomeningeal and perivascular spaces in the brain, in the vicinity of larger blood vessels, participating in cerebrospinal fluid transport and maintaining vascular elasticity (Drieu et al., 2022). Numerous studies have shown that targeting BAMs has beneficial effects on a wide range of diseases. BAMs are involved in amyloid β-induced cerebrovascular oxidative stress and cerebral amyloid angiopathy (Park et al., 2017; Uekawa et al., 2023). In response to ischemic stroke, BAMs attract granulocytes and promote vascular endothelial permeability (Pedragosa et al., 2018; Candelario-Jalil et al., 2022). Thus, inhibiting BAM-induced neuroinflammation is a potential therapeutic approach for ischemic stroke. However, the detailed mechanism by which BAMs induce cerebral injury are still unclear. Thus, comprehensive research into the role of BAMs in ischemic stroke is necessary. In the current study, we performed a comprehensive single-cell RNA sequencing analysis of ischemic stroke using two databases. BAM transcriptome changes in the acute phase of ischemic stroke are characterized by reduced endothelial cell proliferation and enhanced inflammation. Additionally, BAMs are prominent influencers and mediators of tumor necrosis factor (TNF) pathways. BAM inhibitors may attenuate the inflammatory response following ischemic stroke. These inhibitors include Janus kinase inhibitors such as tocilizumab and baricitinib, targeting the interleukin-6 and Janus kinase/STAT pathways, respectively (Obeng et al., 2016; Wang et al., 2024). Monoclonal antibodies, including anti-interleukin-1 and anti-TNF-α, as well as other biologics can also block pro-inflammatory signaling (Zhong et al., 2022). Finally, transforming growth factor-β serves as an immunomodulator, enhancing M2 polarization of BAMs to further mitigate the inflammatory response. Subsequently, we identified critical transcription factors that modulate the response of BAMs to ischemic stroke. The transcriptomic alterations that occur in response to ischemic stroke are orchestrated by complex regulatory networks. Accumulating evidence shows that decreased neutrophil infiltration after cerebral ischemia improves the prognosis of ischemic stroke (Dhanesha et al., 2022; Li et al., 2022). BAMs, which act as a bridge between the brain and the immune system, play an extremely essential role in communication between the brain and immune cells (Coles et al., 2017; De Vlaminck et al., 2022). These results suggest that BAMs recruit myeloid cells and release inflammatory factors to trigger neuroinflammation after ischemic stroke. Accordingly, we propose that BAM depletion eventually results in a decrease in myeloid infiltration and inflammatory factor release, which subsequently mitigates neuroinflammation.

Recent advances in single-cell sequencing analysis have highlighted BAM regulation as a promising therapeutic strategy for ischemic stroke. In this study, we explored the effects of BAM depletion using liposomes containing clodronate on an animal model of stroke. Various parameters were assessed, including cerebral blood flow, the ratio of infarct volume to total brain volume, and neurological function. We also performed immunofluorescence staining, hematoxylin-eosin (HE) staining, and blood biochemical characterization of liver and kidney function. Additionally, we investigated the effects of TNF inhibitor R-7050 injection on stroke outcomes.

Methods

Data sources

A six-sample sham and transient middle cerebral artery occlusion (MCAO) mouse model single-cell RNA sequencing dataset (GSE 174574) (Zheng et al., 2022) was downloaded from the Gene Expression Omnibus (GEO) database (https://www.ncbi.nlm.nih.gov/geo/). Another dataset was obtained from GSE 225948, which included sham and MCAO day 2 group mice (Garcia-Bonilla et al., 2024). A total of ten MCAO mice and nine sham mice were included in our analysis. The datasets we analyzed at 1 and 2 days post-ischemic stroke correspond to the acute phase of stroke.

Single-cell RNA sequencing data quality control and cell type annotation

To remove low-quality cells, we utilized the 'PercentageFeatureSet' function to assess the percentage of mitochondria and ribosomes for each cell. Cells with fewer than 400 features or more than 6000 features were excluded from the analysis. In addition, we retained only those cells that exhibited a mitochondrial percentage of less than 20% combined with a ribosomal percentage of more than 1% for subsequent evaluation. Following the removal of low-quality cells (Hao et al., 2021), we integrated the two single-cell datasets using canonical correlation analysis. We calculated the standard deviation of each gene across all cells and selected the most variable 2000 genes for further evaluation. Then we implemented a resampling test inspired by the JackStraw procedure (Satija Lab, New York City, NY, USA). We randomly permuted a subset of the data (1% by default) and reran the principal component analysis, constructing a 'null distribution' of gene scores, then repeated this procedure. We defined 'significant' principal components as those strongly enriched in low *P*-value genes for downstream clustering and dimensional reduction. Seurat (Satija Lab) analysis was implemented using a graph-based clustering approach (Hao et al., 2024). Distances between the cells were calculated based on previously identified principal components. Briefly, Seurat was used to embed cells in a shared-nearest neighbor graph, with edges drawn between cells via similar gene expression patterns. To partition this graph into highly interconnected quasi-cliques or communities, we first constructed the shared-nearest neighbor graph based on the Euclidean distance in the principal component analysis space and refined the edge weights between any two cells based on the shared overlap in their local neighborhoods (Jaccard distance). We then clustered cells using the Louvain method to maximize modularity. After clustering, we obtained brain cell type markers from CellMarker 2.0 (http://bio-bigdata.hrbmu.edu.cn/CellMarker/) and used them to labeled th clusters (Hu et al., 2023). Finally, we validated the accuracy of our annotations based on the abundance of top five marker genes for each cell type.

Enrichment analysis

We used the 'Findmarkers' function of Seurat to identify signature genes for subsequent analysis (Hao et al., 2021). Enrichment characterized the feature sets using the R package 'clusterProfiler' (Yu et al., 2012). Gene Ontology-biological process (GO-BP), Kyoto Encyclopedia of Genes and Genomes (KEGG), Reactome, and Hallmark database analyses were carried out using the Molecular Signatures Database (MSigDB, https://www.gsea-msigdb.org/gsea/msigdb) (Liberzon et al., 2015).

Gene set enrichment analysis

Differentially expressed genes (DEGs) were identified using the 'Findmarks' function. Then, the obtained DEGs were ranked based on logfc values. Gene sets were acquired from MSigDB (Liberzon et al., 2015). 'ClusterProfiler' was used for geneset enrichment analysis, and the 'gseabase' package was used for visualization.

Cell–cell communication analysis

The Seurat objects were divided into two groups based on their cellular origin for subsequent analyses. Next, we converted the Seurat objects into CellChat objects using the 'creatCellChat' function (Jin et al., 2021), assigning CellChatDB.mouse (https://rdrr.io/github/sqjin/CellChat/man/CellChatDB.mouse.html) as the reference database. A default threshold of 10 was set for screening cell interactions. After constructing the cell communication network, we merged the CellChat objects from the sham and MCAO groups to assess ligand–receptor pairs that exhibited differences in interaction strength and frequency.

High-dimensional weighted gene co-expression network analysis

High-dimensional weighted gene co-expression network analysis (hdWGCNA) was performed to identify key genes associated with macrophages in the MCAO model (Morabito et al., 2023). Macrophage populations were selected from scRNA data, and gene expression correlation matrix, weighted gene co-expression network, and module detection analyses were conducted. Module–trait relationship analysis identified modules significantly associated with the MCAO group, and hub genes within significant modules were identified using the R package 'hdWGCNA' (Morabito et al., 2023).

Identification of various stages of derivation of cell populations

To elucidate the fate determination process of cells and identify key regulatory genes in macrophages in response to stroke, we established a trajectory using the monocle3 package (R software, version: 1.2.9). We employed Uniform Manifold Approximation and Projection (UMAP) for dimensionality reduction, and the 'Plot cell' function was used for visualization of the resulting trajectory.

Pseudotime trajectory evaluation

We performed a 'pySCENIC' analysis to identify BAM transcription factors. We filtered the expression matrix and ran GENIE3 (R software, version: 1.28.0) to obtain the relevance network of transcription factors and potential

targets. Next, potential direct binding targets were identified based on DNA motif analysis. The AUcell function was used to compute transcription factor activities (Aibar et al., 2017).

Middle cerebral artery occlusion procedure

This study was approved by the Ethical Committee of the Affiliated Hospital of Qingdao University on March 23, 2022 (No. AHQU-MAL20220323). All experiments were designed and reported according to Animal Research: Reporting of *In Vivo* Experiments (ARRIVE) guidelines (Percie du Sert et al., 2020). Twenty healthy adult male C57BL/6 mice (20–25 g, ~6 weeks) were purchased from Beijing Vital River Laboratory (Beijing, China; license No. SCXK (Jing) 2021-0006). All mice were housed in ventilated cages with a 12/12-hour light/dark cycle at 25°C with 60% humidity and free access to food and water. The mice were randomly divided into the control (n = 8), treated (n = 8), and R-7050 (n = 4) groups. To establish the focal transient MCAO model, the right middle cerebral artery was blocked for 90 minutes (Tang et al., 2020). First, the mice were anesthetized with 3% isoflurane (Shenzhen Rayward Life Technology Co., LTD, Shenzhen, China) using a gas anesthesia device (Shenzhen Rayward Life Technology Co., LTD), a midline incision was made in the neck, and the subcutaneous tissue was carefully dissected using a stereomicroscope. Then, the common carotid artery, external carotid artery, and internal carotid artery were carefully exposed and separated, ensuring that there was no compression of the trachea or surrounding nerves. A thread plug was inserted into the internal carotid artery through the common carotid artery, which was then tightly secured around the thread plug. After suturing the skin and disinfecting the surgical site, the mice were placed on an electric blanket to maintain their body temperature. After a 90-minute period, the sutures were cut, and the thread plug was gently removed. The common carotid artery stump was then reconnected, and the skin was sutured again, followed by a second round of disinfection. Once the mice regained consciousness and resumed normal breathing, they were returned to their cages for routine feeding. The animals were assessed by researchers blinded to the group assignments.

Ventricular injection

The mice were anesthetized with 3% isoflurane for induction and 1.5% isoflurane for maintenance. The animals were subsequently positioned on a stereotaxic frame to keep their heads fixed. Ophthalmic scissors were used to make a 0.8-cm longitudinal incision on the skin of the head, the periosteal connective tissue was stripped and clipped along the cranial surface with forceps, and the cranial surface was cleaned with a sterile cotton ball, exposing the anterior and posterior fontanelle. The microinjector was fixed, and the Z-axis knob (4.5 units) was adjusted so that the microinjector needle was inserted into the lateral ventricle at a location of 1.49 (X-axis), 0.6 (Y-axis), and 2.2 mm (Z-axis) lateral from the bregma. Next, 5 μL of liposomes containing clodronate (5 mg/mL, Yeasen Biotechnology (Shanghai) Co., Ltd. Shanghai, China; the treated group) or phosphate-buffered saline (PBS; 5 mg/mL, China National Pharmaceutical Group Limited, Beijing, China; the control group) was slowly injected.

Neurological scoring

Neurological behavior was investigated 24 hours after reperfusion by two blinded investigators using Zea–Longa scores (Lu et al., 2024). The scoring criteria were as follows: 1) absence of nerve damage: 0 points; 2) inability to fully extend the contralateral front paw: 1 point; 3) rotation toward the opposite side during crawling: 2 points; 4) tendency to fall toward the opposite side while standing or crawling: 3 points; 5) inability to ambulate independently and loss of consciousness: 4 points. This scoring framework provides a systematic approach to evaluating the neurological functions of the subjects, with higher scores indicating more severe neurological injury.

Cerebral blood flow monitoring

A cerebral blood perfusion imaging system was utilized to monitor local blood perfusion in the brain tissue of mice. After 24 hours of reperfusion following MCAO, the mice were deeply anesthetized by intraperitoneal injection with 1 g/kg tribromoethanol (China National Pharmaceutical Group Limited). After the head was positioned and disinfected, the scalp was opened to expose the skull. The cerebral blood flow at the same localized point for each mouse in both groups was measured using a PeriCam PSI System (Perimed AB, Järfälla, Sweden).

2,3,5-Triphenyltetrazolium chloride staining

2,3,5-Triphenyltetrazolium chloride (TTC) staining of brains collected 24 hours post-reperfusion was performed to assess the infarct volume. The mice were deeply anesthetized by intraperitoneal injection of 1 g/kg tribromoethanol and subsequently euthanized by cervical dislocation. The brains were removed, and two-millimeter coronal brain slices were prepared. The slices were stained with 2% TTC (Solarbio, Beijing, China) at 37°C for 20 minutes and then fixed overnight in 4% paraformaldehyde. The infarcted areas in each slice were measured using ImageJ software (version 1.38, National Institutes of Health, Bethesda, MD, USA) (Schneider et al., 2012).

Immunofluorescence staining

Frozen brain tissue was treated with 0.3% Triton X-100 (Shanghai Aladdin Biochemical Technology Co., LTD., Shanghai, China) for 10 minutes, blocked with 10% bovine serum albumin (Solarbio)-PBS solution for 2 hours, treated with primary antibodies at 37°C for 2 hours, and then treated with secondary antibodies. F4/80 was used to stain for macrophages and ionized calcium binding adaptor molecule 1 (Iba1) was used for microglia (Koneru et al., 2011; Ma et al., 2016). 4′,6-Diaminidine-2-phenylindole (DAPI) staining working solution (Wuhan Sanying Biotechnology Co., LTD., Wuhan, China) was also added dropwise to the samples. After sealing with anti-fluorescence quenching tablets and drying at room temperature for 24 hours, the samples were observed under a confocal microscope (Carl Zeiss, Oberkochen, Germany). ImageJ software was used to analyze the fluorescence intensity of the images. The rabbit anti-STAT3 polyclonal antibody (1:200, Cat# CL488-60199, RRID: AB_2883117), rabbit anti-TNF-α monoclonal antibody (1:200, Cat# CL488-60291, RRID: AB_2883136), rabbit anti-F4/80 polyclonal antibody (1:500, Cat# CL488-28463, UNIPROT ID Q61549), rabbit anti-Iba1 monoclonal antibody (1:500, Cat# 81728-1-RR, UNIPROT ID P55008), and goat anti-rabbit IgG (H+L)-CoraLite-488 antibody (1:200, Cat# SA00013-2, RRID: AB_2797132) were all purchased from Wuhan Sanying Biotechnology Co., LTD.

Hematoxylin-eosin staining

HE staining of brain, heart, liver, spleen, lungs, and kidneys was performed 24 hours post-surgery. After immersed in formalin for 1 week, the organs were embedded in paraffin, sectioned into thin slices and then stained with hematoxylin-eosin (Solarbio).

Biochemical characterization of liver and kidney function via blood parameters

In total, 500 μL of blood was collected from the abdominal aorta in both the control and treated groups 24 hours after surgery and stored at 4°C. Indicators of liver and kidney function, including alanine transaminase, aspartate aminotransferase, alkaline phosphatase, blood urea nitrogen, uric acid, and creatinine were assessed using an automatic biochemical analyzer (BS-360E, Shenzhen Mindray Biomedical Electronics Co., Ltd., Shenzhen, China).

Enzyme-linked immunosorbent assay

In total, 500 μL of blood was collected from the abdominal aorta 3 days after surgery. The plasma levels of TNF-α and STAT3 in both the control and treated groups were detected using enzyme-linked immunosorbent assay (ELISA) kits (Solarbio) according to the manufacturer's instructions.

R-7050 injection

The mice were injected intraperitoneally with R-7050 (5 μg/g; MedChemExpress, Monmouth Junction, NJ, USA) after anesthesia and half an hour before the stroke surgery. Blood flow, TTC staining, and neurological behaviors were evaluated 24 hours post-surgery.

Statistical analysis

Two blinded investigators performed the neurological scoring tests. Two-tailed Student's t-test was performed using GraphPad Prism (version 8.3.0 for Windows, GraphPad Software, Boston, MA, USA, www.graphpad.com). The results are expressed as mean ± standard deviation (SD). A significance level of $P < 0.05$ was considered statistically significant for all data.

Results

Single-cell RNA sequencing uncovers macrophage alterations in ischemic stroke

Myeloid cells, particularly macrophages, play multiple roles in ischemic stroke (Cai et al., 2018, 2019, 2023). To elucidate the diverse functions of

macrophages in ischemic stroke, we conducted canonical correlation analysis (Drieu et al., 2022) by integrating two GEO single-cell datasets (GSE 174574 and GSE 225948), which include samples from ten MCAO mice and nine sham mice. After excluding cells with low RNA abundance or high levels of mitochondrial RNA, we obtained a total of 74,826 cells for subsequent analysis (**Figure 1A**). We visualized both groups of cells using UMAP and found that the batch effect was eliminated in both groups (**Additional Figure 1A**). We adjusted the number of principal components to 30, resulting in the identification of 22 cell clusters at a resolution of 0.8, which were visualized using UMAP (**Additional Figure 1B**). Based on the expression levels of generally recognized markers, we ultimately identified ten cell types (**Figure 1B** and **Additional Figure 2**). These assigned cell types were further validated through their DEGs (**Figure 1C**). As expected, we observed marked changes in the relative proportions of individual cell clusters following acute brain ischemia-reperfusion. Acute ischemic stroke was characterized by an increase in the number of macrophages (**Figure 1D** and **Additional Figure 3**). Macrophages respond robustly to ischemic stroke, significantly infiltrating reperfusion lesions within 24 hours (Blank-Stein and Mass, 2023). To further characterize transcriptional alterations in macrophages during the response to cerebral ischemia-reperfusion, we defined a corrected *P* value of less than 0.05 and a logfc absolute value > 0.25 as the criteria for identifying DEGs (**Figure 1E** and **Additional Table 1**). Enrichment analysis indicated that upregulated genes in ischemic stroke macrophages were associated with regulation of the inflammatory response (**Figure 1F** and **Additional Table 2**). To explore the expression of inflammatory factors by prominent cell types in ischemic stroke, inflammatory pathway genes were identified and inflammation scores were calculated; macrophages exhibited the highest scores (**Figure 1G**). In addition, compared with macrophages in the sham group, the acute ischemic stroke macrophages displayed a higher inflammation score (**Figure 1H**). These results revealed that massive numbers of macrophages invade the brain and participate in activation of the inflammatory response. A previous study demonstrated that elimination of cell death–induced neuroinflammation is a prerequisite for tissue repair in acute ischemic stroke (Cai et al., 2023). Blocking macrophage-induced neuroinflammation, which establishes a stable environment for tissue repair and regeneration, is a promising therapeutic objective in ischemic stroke.

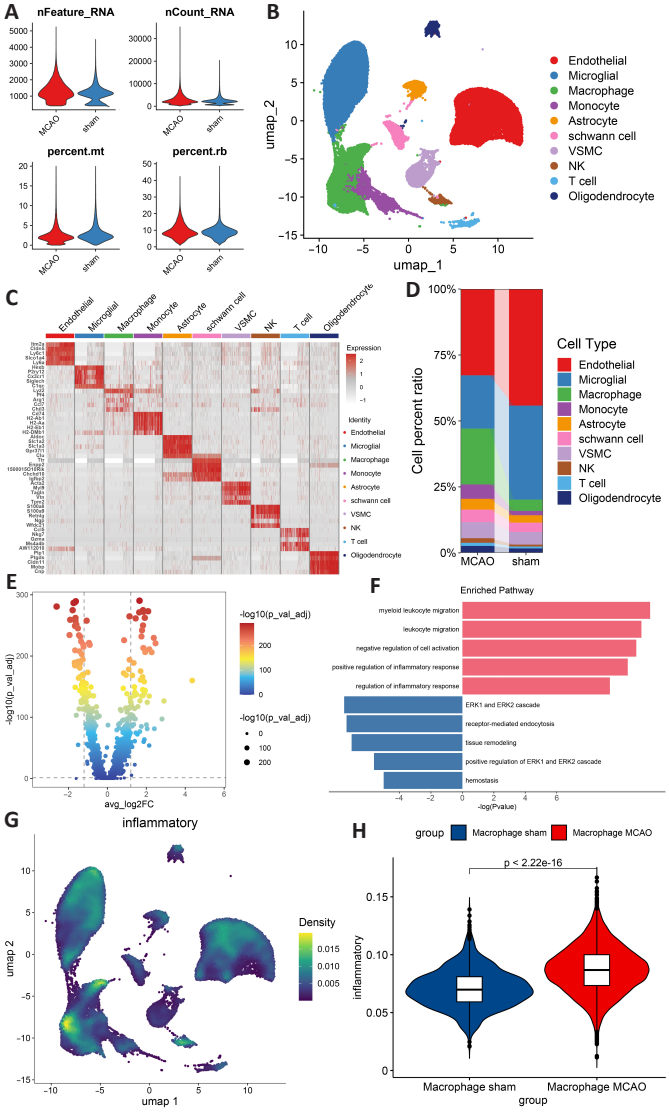

Figure 1 | **Single-cell RNA sequencing uncovers macrophage alterations in ischemic stroke.**

(A) Violin diagram of mitochondrial proportions and ribosomal percentages in the two groups after filtering. (B) Annotation of cell types of the 74,826 cells and visualization with UMAP. (C) Heatmap of marker genes for each cell type. (D) Bar diagram of the proportion of each cell type in the two groups. (E) Macrophage DEGs between the sham and MCAO groups. (F) Enrichment analysis of macrophage DEGs in MCAO group. (G) Density plot of scores for an inflammatory gene set. (H) Differences in macrophage inflammatory scores between the two groups. DEGs: Differential expressed genes; MCAO: middle cerebral artery occlusion; UMAP: Uniform Manifold Approximation and Projection.

Border-associated macrophage heterogeneity in ischemic stroke

Accumulating evidence suggests that, in response to ischemic stroke, the genetic profile of BAMs undergoes significant alterations, which strongly impacts the integrity of the blood–brain barrier (DeLong et al., 2022). However, the specific transcriptional changes in BAMs and the underlying mechanism of their response to ischemic stroke remain unclear. BAMs can be distinguished from microglia by their localization and by expression of the cell surface marker mannose receptor C-type 1 (Mrc1) (Goldmann et al., 2016). To elucidate shifts in transcriptional signatures associated with ischemic stroke at the single-cell level, we re-clustered the macrophages into seven distinct clusters (**Figure 2A** and **B**: MHCII mac (markers: H2-Eb1, H2-Aa), Ly6c mac (markers: Hp, Pac8), Fabp5 mac (markers: Fabp5, Gpnmb), Mrc1 mac (markers: Mrc1, Pf4), Spp1 Mac (markers: Arg1, Cxcl2, Spp1), Cxcl10 mac (markers: Cxcl10, Rsad2), and Cxcl2 mac (markers: S100a8, S100a9)). To determine the possible functional heterogeneity of Mrc1 mac between the sham and MCAO groups, we performed Gene Ontology (GO) and Gene Set Enrichment Analysis (GSEA) analyses. Inflammatory mediator release and immune cell recruitment were observed in the MCAO group (**Figure 2C**), while Mrc1 mac in sham mice was predominantly enriched in regulatory genes including those involved in the ERK1/2 cascade and in endothelial cell proliferation (**Figure 2D**).

These data indicate that Mrc1 macrophages, which are the most prevalent macrophages in a homeostatic state, play a critical role in maintaining vascular integrity, primarily by regulating endothelial cell proliferation. However, during ischemic stroke, the function of Mrc1 macrophages shifts, and they release inflammatory mediators, thereby inducing neuroinflammation by attracting myeloid cells and neutrophils (**Figure 2D** and **Additional Figures 4**, and **5**). Furthermore, in addition to chemokines, the expression of core indicators of vascular leakage and the extracellular matrix, such as vascular endothelial growth factor A (Vegfa), hypoxia inducible factor 1 subunit alpha (Hif1a), matrix metallopeptidase 8 (Mmp8), and matrix metallopeptidase 8 (Mmp12), were elevated in MCAO Mrc1 macrophages (**Figure 2E**). All of these results indicate that Mrc1 mac affects the outcome of ischemic stroke through multiple biological effects, thereby providing a potential target for the treatment of ischemic stroke.

Distinct cellular interaction patterns in middle cerebral artery occlusion and sham mice

Next we performed a cellular communication analysis to compare different patterns of cell–cell communication in the context of ischemic stroke and homeostasis. We established a ratio of the combined pathway probabilities > 1.05 and a *P* value < 0.05 as the thresholds for identifying differentially activated pathways. The frequency and strength of the interactions between macrophages and endothelial cells were significantly down-regulated in the MCAO group compared with the sham group (**Figure 3A** and **B**), which is consistent with a previous study (Candelario-Jalil et al., 2022). We tested the distinct patterns of cellular interactions between the two groups (**Figure 3C**). As TNF expression is the core signature of inflammation, blocking TNF can alleviate numerous inflammatory diseases (Bradley, 2008). Several studies have shown that inhibiting the release of inflammatory factors, such as TNF, effectively attenuates stroke-induced neuroinflammation (Liguz-Lecznar et al., 2015; Prescott et al., 2023; Soldatos et al., 2023; Ren et al., 2024). To identify distinct cell–cell communication patterns in BAMs, we extracted Mrc1 mac cells and compared their interaction patterns. Compared with those in

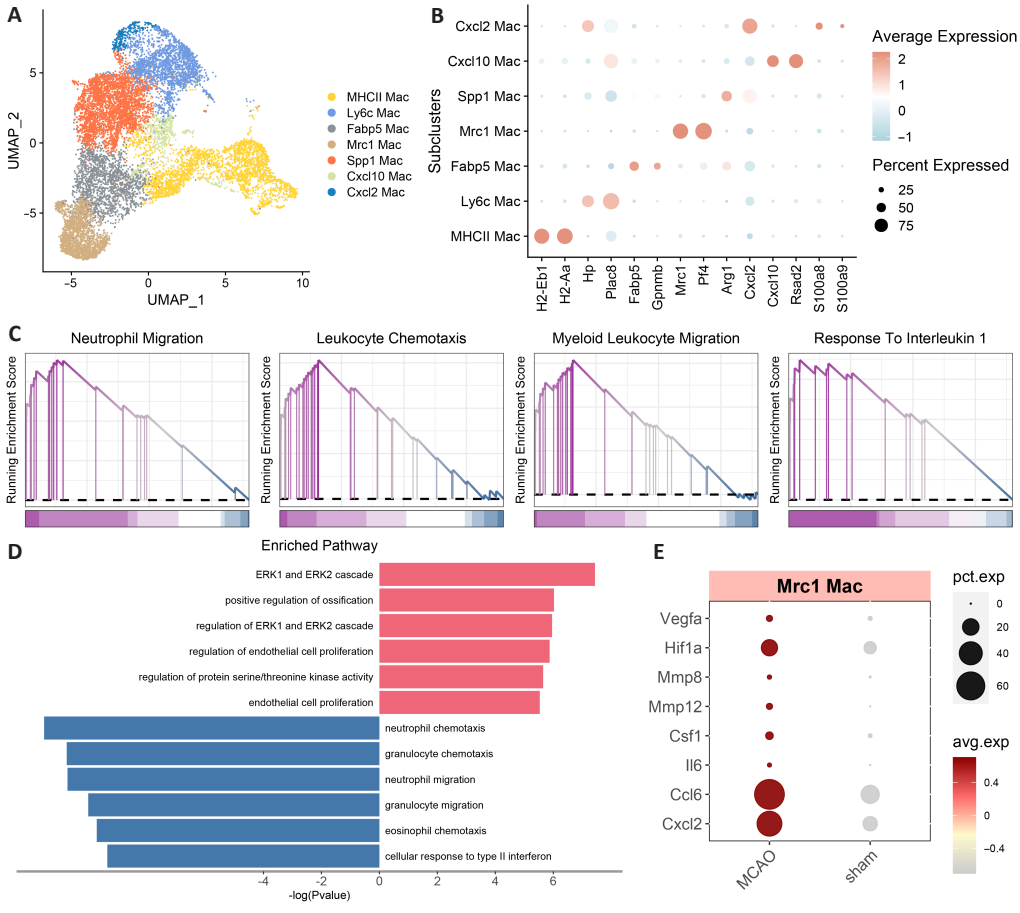

Figure 2 | BAM heterogeneity in ischemic stroke.
(A) Annotation of macrophage cluster cell types. (B) Dot plot of marker genes for each macrophage cluster. (C) Mrc1 macrophage GSEA results after ischemic stroke. (D) Enrichment analysis of Mrc1 macrophage DEGs in the sham group (*vs.* the MCAO group). (E) Dot plot illustrating vascular leakage–and extracellular matrix–related genes. BAM: Border-associated macrophage; DEGs: differential expressed genes; GSEA: Gene Set Enrichment Analysis; MCAO: middle cerebral artery occlusion.

sham mice, inflammation-related ligand–receptor pairs, such as TNF, C–C motif ligand (CCL), and macrophage migration inhibitory factor (MIF), were obviously enriched in Mrc1 macrophages following MCAO (**Figure 3D**). In the context of ischemic stroke, Mrc1 macrophages served as critical activators of TNF signaling (**Figure 3E** and **F**). Furthermore, we found that, during ischemic stroke, Mrc1 macrophages not only sent and received TNF signals, but also functioned as the most crucial regulators and influencers of this pathway (**Figure 3G**). We also found that TNF signaling was predominantly mediated by the Tnf and TNF receptor superfamily member 1A (Tnfrsf1a) receptor–ligand pair (**Additional Figure 6**). Consistent with the CellChat results, the abundance of Tnf core signatures was upregulated in macrophages in the context of ischemic stroke (**Figure 3H**).

hdWGCNA identified core Mrc1 macrophage signatures related to inflammation

To characterize the hub signatures of Mrc1 macrophages, we performed hdWGCNA. To establish a scale-free macrophage network, we selected 3 as the soft threshold (**Figure 4A** and **B**). The genes were classified into six modules; the brown modules predominantly mapped onto Mrc1 macrophages and ischemic stroke (**Figure 4C**, **Additional Figure 7** and **Additional Table 3**). Subsequently, brown module gene activities among all macrophages were measured using the AUcell function. The results showed that Mrc1 macrophages had the highest score (**Figure 4D** and **E**). In addition, we constructed a protein–protein interaction network, which suggested communication among the hub genes in brown module (**Figure 4F**). Crucial transcription factors that regulate the inflammatory response, such as Jun proto-oncogene (Jun), early growth response 1 (Egr1) (Drieu et al., 2022) and CD81 antigen (Cd81), were located at the core of the network. Next, we performed multiple enrichment analysis and found that these genes were mainly enriched in the Tnf and neuroinflammation associated pathways (**Figure 4G**). In summary, we identified the Mrc1 macrophage module and found that its hub genes are related to inflammation.

pySCENIC analysis of regulatory transcription factors

We established a transcription factor regulatory network to determine whether Mrc1 macrophage cell fate is reversible between homeostasis and ischemic stroke. Using AUCell, we computed transcription factor reactivity and observed that the activities of signal transducer and activator of Stat3, myelocytomatosis oncogene (Myc), and nuclear factor interleukin 3 regulated (Nfil3) were clearly increased (**Figure 5A**). Stat3 and Nfil3 participate in cerebral inflammation after ischemic stroke (Wang et al., 2022; Zhang et al., 2023b). Therefore, targeting Stat3 may present a promising therapeutic avenue for mitigating Mrc1 macrophage–induced neuroinflammation. To further characterize the distinct fates of macrophages, we employed pseudotime trajectory evaluation to infer macrophage transitions post-ischemic stroke. Considering MHC II macrophages as the origin of the pseudotime trajectory, we observed the transition states of macrophages in pseudotime and in different cell types (**Figure 5B** and **C**). We observed that Tnf and the critical transcription factor Stat3 were overexpressed in Mrc1 macrophages (**Figure 5D** and **E**).

Border-associated macrophage depletion protects against acute stroke

We subjected 20, 6-week-old mice to transient MCAO. Mrc1 macrophages can be depleted by intracerebroventricular injection of liposomes containing clodronate (Hawkes and McLaurin, 2009; Faraco et al., 2016). Therefore, we randomly divided the mice into two groups and injected them with liposomes containing clodronate (treated group) or PBS (control group). All mice were assessed for indicators of stroke (**Figure 6A**). The cerebral blood perfusion images showed more blood flow in the treated group than in the control group within 60 seconds (**Figure 6B**). Compared with the control group, TTC staining showed smaller white areas in the brain, with clearly decreased infarct volume, in the treated group (**Figure 6C** and **D**). Moreover, the mice in the depletion group exhibited significant improvements in neurological scores, indicating that injecting liposomes containing clodronate exerted a positive effect on neurological status (**Figure 6E**). Immunofluorescence staining showed that TNF and F4/80 expression levels were decreased (**Figure 6F** and **Additional Figures 8** and **9**), while there was no significant change in STAT3 expression (**Figure 6F** and **Additional Figure 10**). In addition, TNF and STAT3 plasma levels increased 3 days post-surgery, potentially indicating systemic inflammation triggered by the injury (**Figure 6G**). Liver- and kidney-related blood biochemical characterization indicated no significant side effects (**Additional Figure 11**).

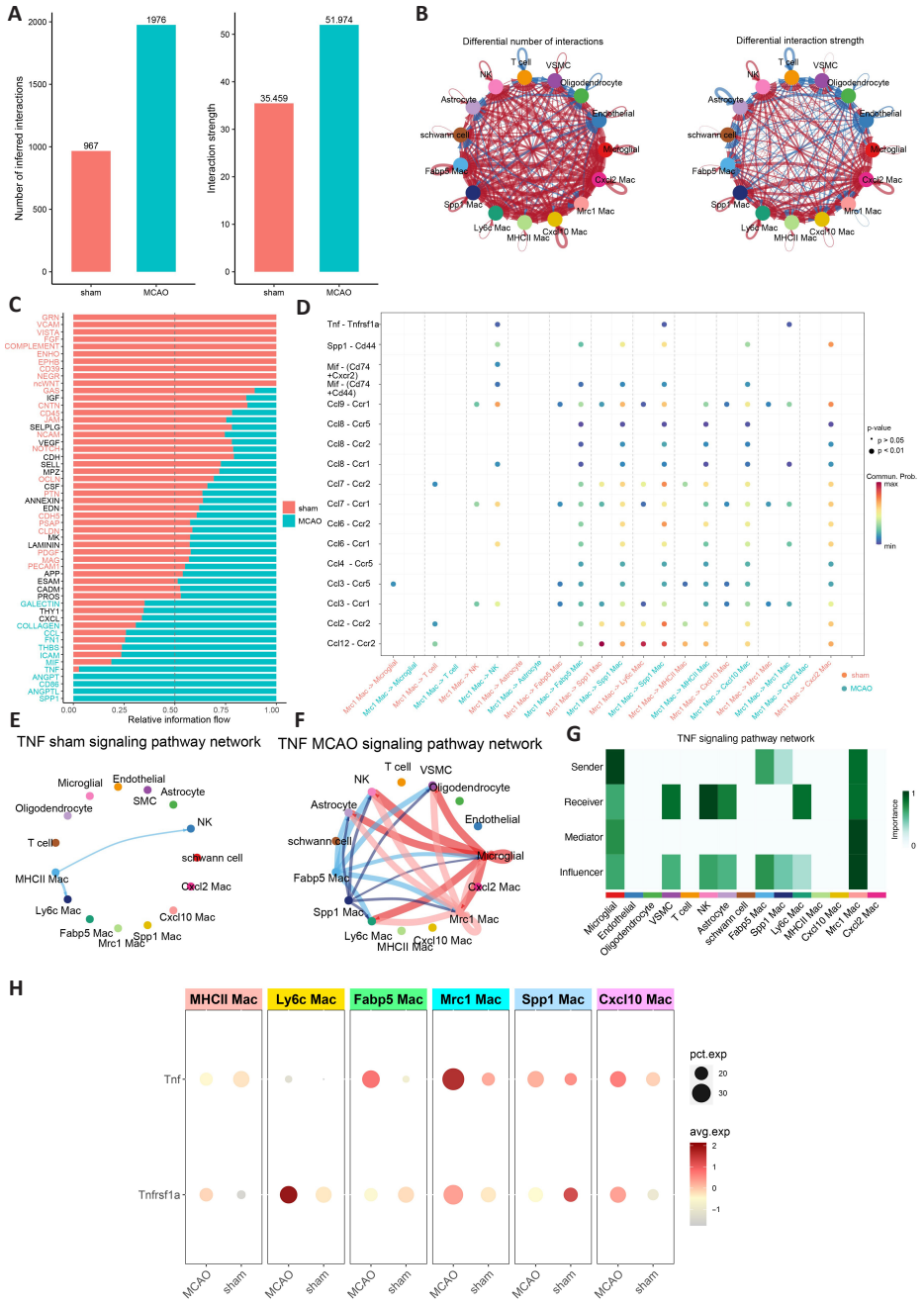

Figure 3 | Distinct cellular interaction patterns in MCAO and sham mice.

(A) Differences in the number of interactions or strength of interactions among different cell populations in the sham and MCAO groups. (B) Circle diagrams for the MCAO group indicating differences in the number and strength of interactions among different cell types. (C) Important signaling pathways were ranked based on the difference in overall information flow between the inferred sham and MCAO networks. The top signaling pathways indicated in red were enriched in the sham group, while those in green were enriched in the MCAO group. (D) Bubble diagram of upregulated and downregulated ligand–receptor pairs in Mrc1 macrophages. (E) The TNF pathway network in the sham group. (F) The TNF pathway network in the MCAO group. (G) Dot plot illustrating the leading participants in the TNF signaling pathway in the MCAO group. (H) Dot plot of Tnf and Tnfrsf1a expression levels among all MCAO macrophage clusters. MCAO: Middle cerebral artery occlusion; TNF: tumor necrosis factor; Tnfrsf1a: tumor necrosis factor receptor superfamily member 1A.

To investigate the effect of clodronate-containing liposomes on microglia, Iba1 staining of brain tissue was performed 24 hours post-surgery. The immunofluorescence images revealed the presence of microglia both with and without treatment, and no significant differences were observed between the groups. Therefore, it can be concluded that clodronate-containing liposomes primarily impact BAMs without significantly affecting the number of microglia (**Figure 7A**). Meanwhile, HE staining of the brain demonstrated relatively few inflammatory cells in the cerebral infarction area following treatment, indicating recovery (**Figure 7B**). Additionally, there were no significant differences in the number of inflammatory cells preset in the heart, liver, spleen, lungs, and kidneys before and after treatment (**Figure 7C**).

Next, we utilized TNF inhibitors to confirm the beneficial effect of TNF reduction on recovery from cerebral infarction. Cerebral blood perfusion images showed a large red area, indicating improved blood flow after treatment with R-7050 (**Figure 8A**). Compared with the control group, TTC staining revealed a smaller white area in the brain and a notable reduction in infarct volume in the treated group (**Figure 8B** and **C**). However, there were no significant differences observed in the behavioral performance of the mice 24 hours after surgery (**Figure 8D**).

Discussion

Macrophages exhibit diverse effects in cerebral ischemic stroke (Cai et al., 2018, 2019). They can either exacerbate neuroinflammation by secreting pro-inflammatory cytokines or promote tissue regeneration (Cai et al., 2019; Zhang et al., 2024, 2025). To determine whether distinct macrophage transcription profiles contribute to neuroinflammation, we conducted a comprehensive single-cell analysis of macrophages in the context of ischemic stroke. Our analysis revealed that macrophages significantly infiltrated the injury site and displayed the highest inflammatory scores among all cell types following stroke.

While the majority of macrophages remain in a homeostatic state, BAMs play a crucial role in maintaining this homeostasis (Mrdjen et al., 2018; Pedragosa et al., 2018; Cai et al., 2019). Perivascular macrophages, a subset of BAMs, are not only found in the central nervous system, but also in the blood vessels of other organs (e.g., skin, peritoneum, and inner ear), where they have been shown to regulate barrier integrity (Hoffmann and Miron, 2024). Previous studies have reported that BAMs are a therapeutic target for Alzheimer's disease and septic heart disease (Drieu et al., 2022; Zhang et al., 2023a). Consistent with earlier findings, under homeostatic conditions, we found that BAMs were involved in

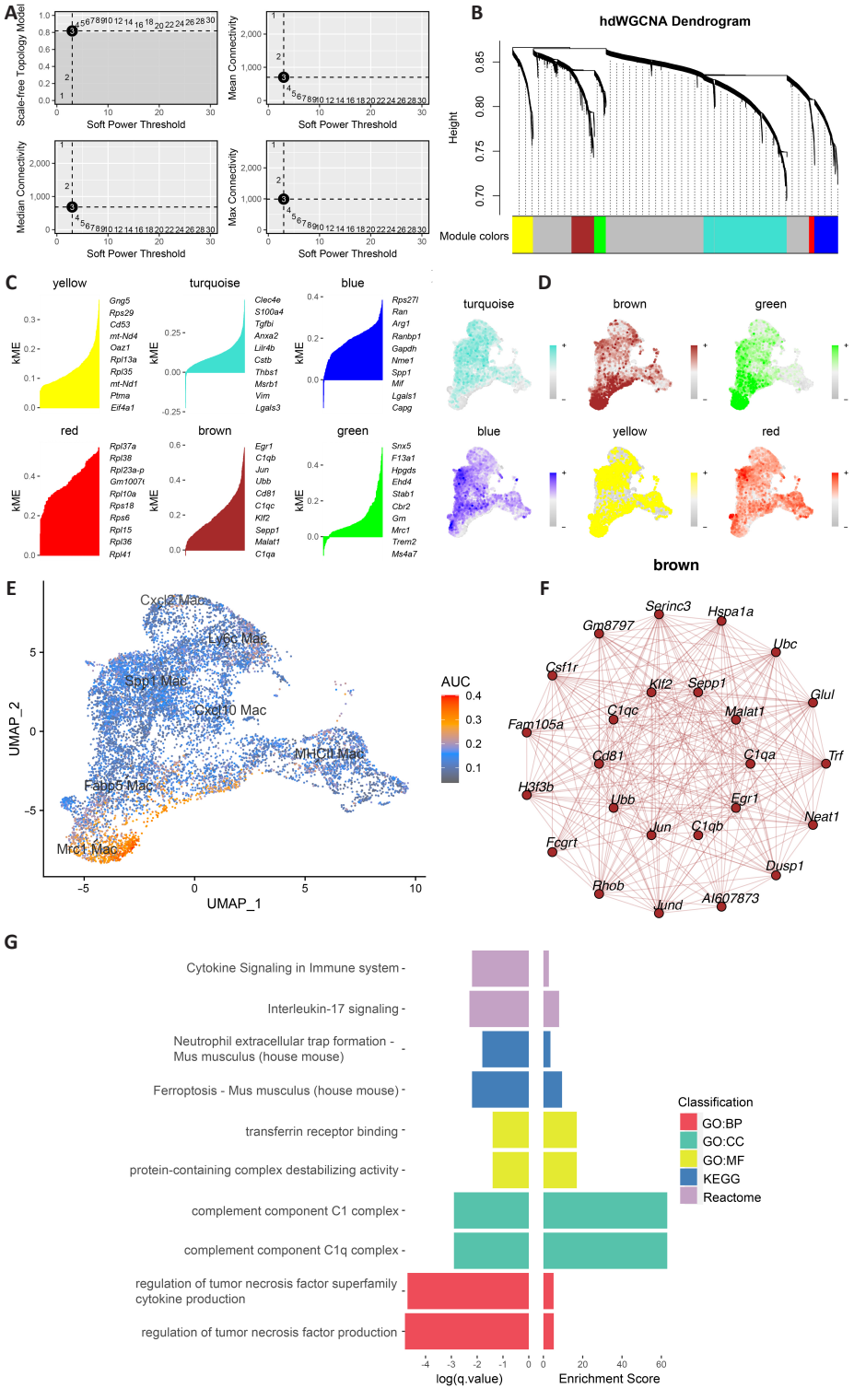

Figure 4 | **HdWGCNA identified core signatures of Mrc1 macrophages related to inflammation.** (A, B) Weighted gene co-expression network analysis of macrophages was performed. (C) The first 10 eigengenes of each module were ranked by eigengene-based connectivity (kME). (D) UMAP analysis of the expression of each module among all macrophages. (E) UMAP analysis of the expression of the brown module among all macrophages. (F) Protein–protein interaction network of the brown module. (G) Enrichment analysis of the brown module. HdWGCNA: High-dimensional weighted gene co-expression network analysis; UMAP: Uniform Manifold Approximation and Projection.

regulating endothelial proliferation and preserving vascular integrity (**Figure 2D**). However, following ischemic stroke, BAMs shift their role, compromising the continuity of cerebral vessels (Pedragosa et al., 2018). Further investigation is needed to elucidate the detailed mechanisms underlying BAM functions after stroke. Single-cell RNA sequencing has provided a novel platform for studying the transcriptional changes in BAMs post-ischemic stroke. Our study revealed a previously unrecognized function of BAMs in this context. We conducted a comprehensive single-cell analysis of BAMs, which we defined as Mrc1 macrophages. In response to hypoxia, the BAM gene expression profile changed, resulting in the secretion of various inflammatory factors. The GSEA results suggested that BAMs are involved in neutrophil chemotaxis and recruit myeloid cells. We believe that myeloid cell and neutrophil inflammation during the acute period of ischemic stroke may be initiated by altered BAM expression profiles. In the acute phase of cerebral stroke, the percentage of BAMs obviously decreased, although the total quantity of BAMs did not change significantly (**Additional Figure 12**). This may be associated with BAM-driven myeloid and neutrophil chemotaxis in the acute phase. Previous research has suggested that peripheral vascular macrophage exhaustion potentially decreases neutrophil numbers in a mouse model of bacterial skin infection (Abtin et al., 2014). Another study found that depletion of macrophages with clodronate-carrying liposomes reduced recruitment of neutrophils to the peritoneal cavity after lipopolysaccharide stimulation (De Filippo et al., 2013).

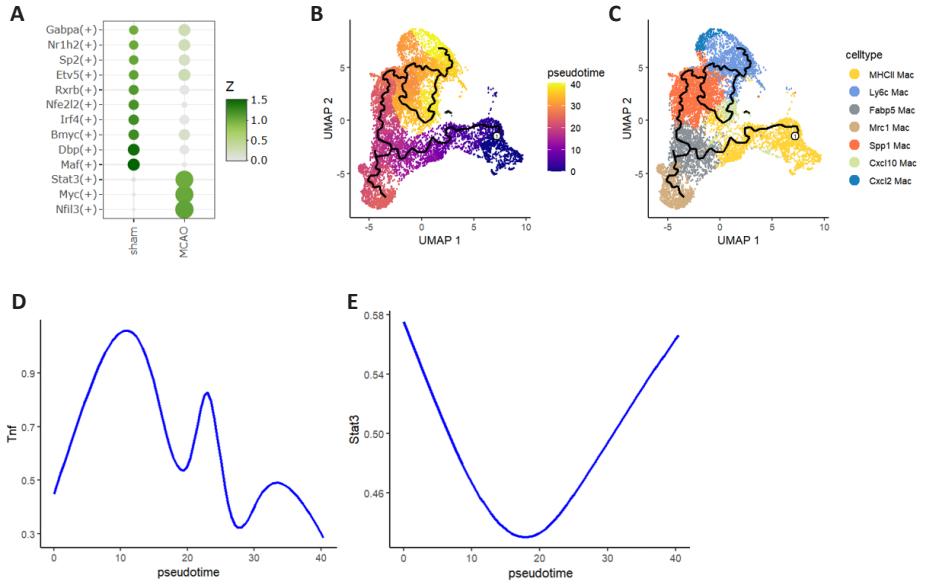

Figure 5 | pySCENIC analysis showing distinct transcription factor regulation.

(A) Dot plot of the transcription factor activities of Mrc1 macrophage. (B, C) Pseudotime trajectory of macrophages. (D, E) The expression levels of Tnf and Stat3 followed by pseudotime trajectory. Stat3: signal transducer and activator of transcription 3; Tnf: tumor necrosis factor.

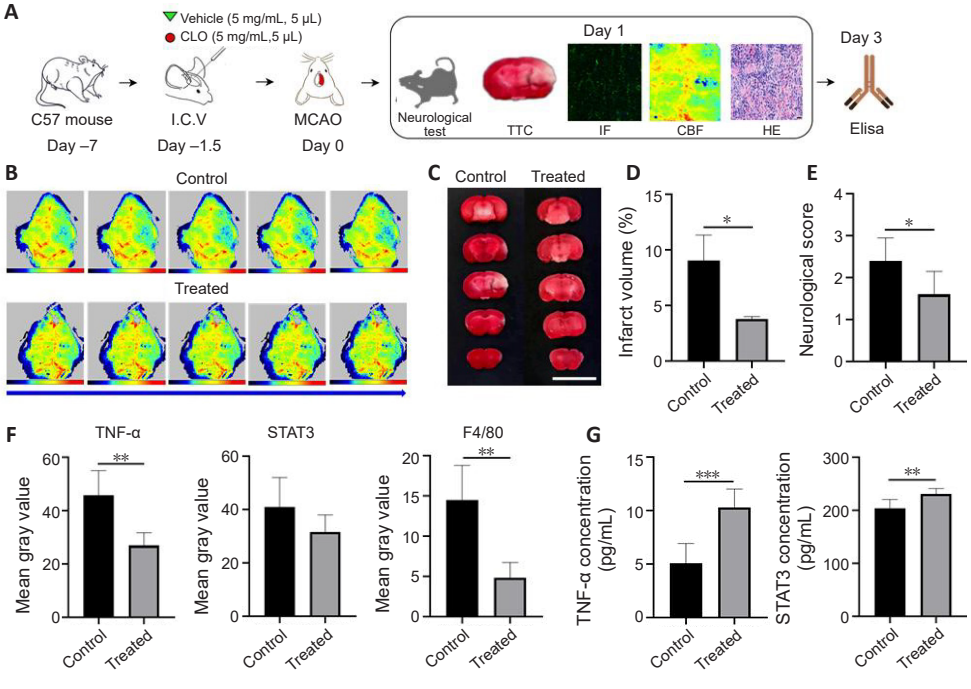

Figure 6 | BAM depletion protects against acute stroke.

(A) Flowchart of the experimental design. (B) Cerebral blood perfusion images of the brain within 60 seconds in the control and treated groups 24 hours after surgery. Less blue color in the right zone of brain in the treated group indicates better blood flow compared with the control group. (C) TTC staining images of brain from the control and treated groups 24 hours after surgery. Less white color was observed in the right brain zone of the treated group compared with the control group. Scale bars: 1 cm. (D) Infarct volume was quantified by TTC staining. (E) Neurological scores were assessed at 24 hours in the control and treated groups. (F) TNF-α, STAT3, and F4/80 immunopositivity in the control and treated groups 24 hours after surgery. (G) ELISA of TNF-α and STAT3 plasma levels 3 days after surgery. Data are expressed as mean ± SD (n = 4 in both groups). *P < 0.05, **P < 0.01, ***P < 0.001 (two-tailed Student's t-test). BAM: Border-associated macrophage; CBF: cerebral blood flow; ELISA: enzyme linked immunosorbent assay; HE: hematoxylin-eosin staining; IF: immunofluorescence staining; STAT3: signal transducer and activator of transcription 3; TNF: tumor necrosis factor; TTC: 2,3,5-triphenyltetrazolium chloride.

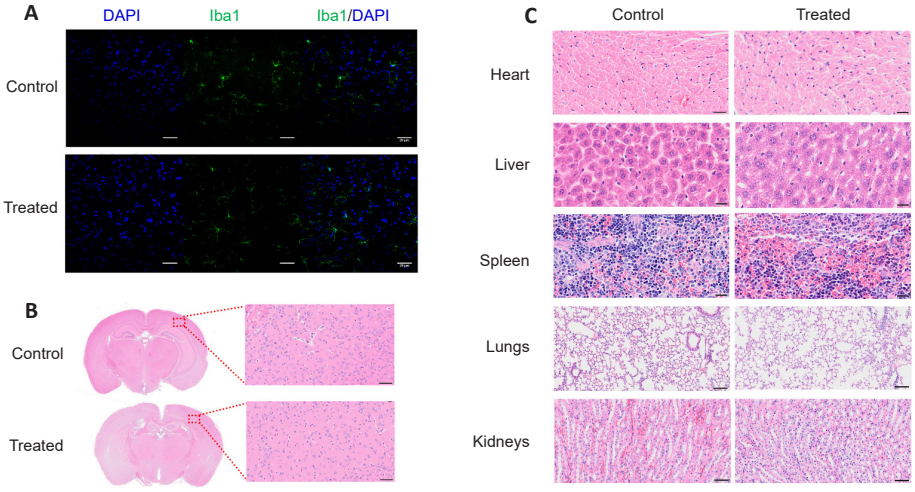

Figure 7 | BAM depletion improves tissue damage after acute stroke.

(A) Immunofluorescence staining for Iba1 (green, stained by CoraLite® 488, CL488) and DAPI (blue) in control and treated mice 24 hours after surgery. No significant differences were found between the two groups (n = 4 in both groups). Scale bars: 20 μm. (B) HE staining of brain tissue from control and treated mice at 24 hours post-surgery. No significant differences were found between the two groups. Scale bars: 20 μm. (C) HE staining of various organs in the control and treated mice at 24 hours post-surgery. No significant differences were found between the two groups. Scale bars: 20 μm. BAMs: Border-associated macrophages; DAPI: 4′,6-diaminidine-2-phenylindole; HE: hematoxylin-eosin; Iba1: ionized calcium binding adaptor molecule 1.

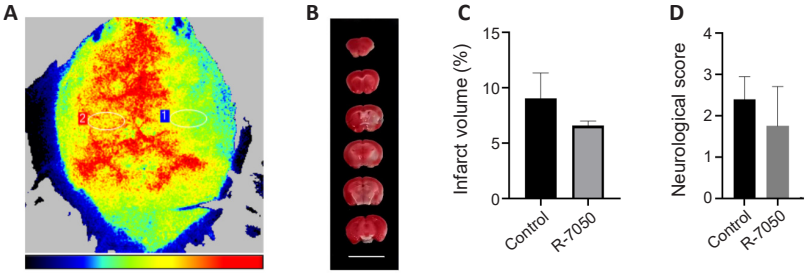

Figure 8 | R-7050 protects against acute stroke.
(A) Cerebral blood perfusion image of the brain in the R-7050-injected group. (B) TTC staining of the brain in the R-7050-injected group. Scale bar: 1 cm. (C) Infarct volume was quantified with TTC staining (n = 4 in both groups). (D) Neurological scores were assessed at 24 hours with or without R-7050 treatment. Data are expressed as mean ± SD and were analyzed by two-tailed Student's t-test. TTC: 2,3, 5-triphenyltetrazolium chloride.

To characterize the global interaction network among brain resident cells and BAMs, we performed CellChat analysis based on gene expression levels in each cell type. Our results suggested that, after stroke, TNF signaling pathways were significantly activated in BAMs, microglia, and natural killer cells. TNF abundance in the acute phase of cerebral stroke is closely related to patient outcome (Liguz-Lecznar et al., 2015; Ye et al., 2020; Soldatos et al., 2023). Blocking acute-phase TNF release effectively improves the prognosis of cerebral stroke (Soldatos et al., 2023). In addition to receiving and sending TNF signals, BAMs are essential regulators and influencers of the TNF signaling pathway after stroke. The results from our animal experiments support this finding. When BAM numbers were reduced (as indicated by decreased F4/80 staining) in the MCAO model, TNF abundance was also moderately reduced either. Administration of clodronate decreased infarct volume and increased behavioral performance in a 6-week mouse model of MCAO. Injection with TNF inhibitors also improved cerebral infarction. Taken together, our findings revealed that, after stroke, BAMs activated the inflammatory response by regulating TNF signaling. BAM depletion inhibited immune cell infiltration and decreased the release of inflammatory factors, which eventually led to improve outcomes and reduce disability rates after cerebral stroke.

A previous study reported that temporary depletion of BAMs only improved the neurological scores in severe MCAO mice (Pedragosa et al., 2018). Another study reported that BAM depletion effectively relieved alcohol-induced ischemic stroke (Drieu et al., 2020). The efficacy of BAM inhibitors may be associated with the severity of stroke. We constructed a mouse model of minor ischemic stroke and administered a BAM inhibitor. The results showed that injecting liposomes containing clodronate for 36 hours clearly reduced the infarct volume. Activated BAMs compromise the integrity of the blood–brain barrier by releasing inflammatory factors and reactive oxygen species (Anfray et al., 2024). BAM depletion has been shown to reduce vascular permeability (Drieu et al., 2022). Therefore, depleting BAMs preemptively may influence infiltration of peripheral blood monocytes into the brain parenchyma. Furthermore, our findings align with previous research indicating that injecting liposomes containing clodronate into the lateral ventricle does not significantly affect the number of microglia (Han et al., 2019; Császár et al., 2022). Due to its complexity and the risk of postoperative injuries, localized cerebral injection is rarely performed in the clinic (Faraco et al., 2016). In addition, enrichment analysis indicated that, during the recovery phase of cerebral stroke, BAMs decreased the signals of inflammatory-related pathways and participated in the maintenance of vessel integrity (**Additional Figure 13**). These findings suggested that BAMs have a sophisticated function during the acute and recovery phases of cerebral stroke. BAM depletion alone did not improve stroke outcomes because of its complex function during the acute and recovery phases. A major challenge of BAMs is that they should counteract deleterious post-ischemic inflammation but retain reparative function.

Transcription factors recognize specific DNA sequences to regulate chromatin structure and transcription, thereby forming complex systems that govern gene expression across the genome. These factors often function as master regulators that orchestrate biological processes such as cell fate determination, developmental patterns, and the regulation of specific signaling pathways. We performed 'pySCENIC' analysis to identify key transcription factors that determine BAM cell fate after stroke. STAT3/HIF-1A signaling is involved in triggering inflammation in acute phase of stroke (Jin et al., 2022; Wang et al., 2022). Acute inhibition of STAT3 improved neurological function scores and reduced infarct volume after cerebral stroke, and macrophages played an important role in this process (Zhu et al., 2021; Wang et al., 2022). In the context of inflammatory diseases, such as apical periodontitis, resident macrophage polarization is partly attributed to the activation of STAT3 signaling (Chen et al., 2022). STAT3 inhibition may be a promising strategy for preventing BAM-induced neuroinflammatory alterations after stroke. We did not detect any significant difference in STAT3 immunofluorescence staining, which may be related to the selection of time points and needs to be further investigated.

There were several other limitations in our study. Firstly, the single-cell RNA sequencing data were obtained from a public database that contains only mouse stroke data, as it is difficult to obtain relevant clinical data and samples. The transcriptional alterations that occur in BAMs after stroke in humans remain to be further investigated. Another major limitation of this study is that it did not investigate the relationship between different dosing times and different time points after stroke. Thus, the ongoing evolution and diversity of BAMs are still unknown.

Our study demonstrates that BAM clearance through clodronate liposomes can effectively reduce both the volume and severity of stroke, thereby offering a promising therapeutic pathway for neuroprotection. Despite these promising results, this treatment strategy has several limitations. Regarding specificity, while clodronate liposomes are designed to specifically target BAMs, their clearance may inadvertently affect the functionality of other immune cell populations, potentially resulting in adverse immune responses. Another concern is the therapeutic window, as the efficacy of this intervention may be constrained by a limited treatment time window; delays in intervention could diminish the therapeutic benefits. Furthermore, regarding cellular regeneration, following the removal of macrophages, it is crucial to investigate strategies to promote the regeneration and repair of brain tissue, as a deficiency in cellular populations could lead to negative outcomes. Individual variability is another concern, as variations in the physiological and pathological profiles of patients can influence their responses to clodronate liposome therapy.

In summary, we integrated single-cell sequencing data from two MCAO mouse datasets and illustrated the transcriptional evolution of BAMs after ischemic stroke. We established a BAM communication and transcription factor network, which provided new insight into BAM-induced inflammation after cerebral stroke. Finally, limitations in the use of BAM depletion for the treatment of brain stroke were identified. Liposomes containing clodronate are a promising therapeutic strategy for BAM-induced neuroinflammation and reduce ischemia–reperfusion injury.

Acknowledgments: *We are grateful to Boyi Ma of The Affiliated Hospital of Qingdao University for his advice and assistance in bioinformatics analysis.*
Author contributions: *NY: conceptualization, data curation, funding acquisition, investigation, project administration, writing-original draft, and writing-review and editing; YZ: conceptualization, data curation, formal analysis, resources, software, writing-original draft, and writing-review and editing; PW: investigation, methodology, project administration, resources, supervision, and writing-review and editing; FZ: data curation, formal analysis, investigation, project administration, resources, and writing-review and editing; CW: investigation, methodology, project administration, resources, validation, visualization, and writing-review and editing; SW: conceptualization, methodology, project administration, funding acquisition, resources, and writing-review and editing. All authors approved the final version of this manuscript.*
Conflicts of interest: *The authors declare that the research was conducted in the absence of any commercial or financial relationships that could be construed as a potential conflict of interest.*

Data availability statement: *All data relevant to the study are included in the article or uploaded as Additional files. Further inquiries can be directed to the corresponding authors.*

Open peer reviewer: *Rui Sun, Washington University School of Medicine in St. Louis, USA; Fangfang Cao, National University of Singapore, Singapore; Rajiu Venkatesan, Mallinckrodt Institute of Radiology, USA.*

Additional files:

Additional Figure 1: *The 74,826 cell annotations and clusters are visualized with UMAP.*

Additional Figure 2: *The 74,826 cell type annotations divided by group.*

Additional Figure 3: *The proportion of macrophages in the two groups.*

Additional Figure 4: *The proportions of each macrophage cluster in the two groups.*

Additional Figure 5: *The proportions of Mrc1 macrophage in the two groups.*

Additional Figure 6: *Contributions of each ligand–receptor pair to the TNF pathway.*

Additional Figure 7: *The relationship between each module and ischemic stroke.*

Additional Figure 8: *Immunofluorescence staining for DAPI (blue) and TNF (green, stained by CL488) in the control and treated groups.*

Additional Figure 9: *Immunofluorescence staining for DAPI (blue) and F4/80 (green, stained by CL488) in the control and treated groups.*

Additional Figure 10: *Immunofluorescence staining for DAPI (blue) and STAT3 (green, stained by CL488) in the control and treated groups.*

Additional Figure 11: *Blood biochemical characterization of liver and kidney.*

Additional Figure 12: *The number of cells in each macrophage cluster in the sham and MCAO groups.*

Additional Figure 13: *The GSEA results show distinct BAM profiles in the acute and recovery phases of ischemic stroke.*

Additional Table 1: *The DEGs of macrophages between sham and MCAO groups.*

Additional Table 2: *Gene Ontology Biology Process enrichment analysis of macrophage DEGs between the sham and MCAO groups.*

Additional Table 3: *The module eigengene-based connectivity of each gene among all the models.*

Additional file 1: *Open peer review reports 1–3.*

References

Abtin A, Jain R, Mitchell AJ, Roediger B, Brzoska AJ, Tikoo S, Cheng Q, Ng LG, Cavanagh LL, von Andrian UH, Hickey MJ, Firth N, Weninger W (2014) Perivascular macrophages mediate neutrophil recruitment during bacterial skin infection. Nat Immunol 15:45-53.

Aibar S, González-Blas CB, Moerman T, Huynh-Thu VA, Imrichova H, Hulselmans G, Rambow F, Marine JC, Geurts P, Aerts J, van den Oord J, Atak ZK, Wouters J, Aerts S (2017) SCENIC: single-cell regulatory network inference and clustering. Nat Methods 14:1083-1086.

Anfray A, Schaeffer S, Hattori Y, Santisteban MM, Casey N, Wang G, Strickland M, Zhou P, Holtzman DM, Anrather J, Park L, Iadecola C (2024) A cell-autonomous role for border-associated macrophages in ApoE4 neurovascular dysfunction and susceptibility to white matter injury. Nat Neurosci 27:2138-2151.

Blank-Stein N, Mass E (2023) Macrophage and monocyte subsets in response to ischemic stroke. Eur J Immunol 53:e2250233.

Bradley JR (2008) TNF-mediated inflammatory disease. J Pathol 214:149-160.

Cai W, Liu S, Hu M, Sun X, Qiu W, Zheng S, Hu X, Lu Z (2018) Post-stroke DHA treatment protects against acute ischemic brain injury by skewing macrophage polarity toward the M2 phenotype. Transl Stroke Res 9:669-680.

Cai W, Hu M, Li C, Wu R, Lu D, Xie C, Zhang W, Li T, Shen S, Huang H, Qiu W, Liu Q, Lu Y, Lu Z (2023) FOXP3+ macrophage represses acute ischemic stroke-induced neural inflammation. Autophagy 19:1144-1163.

Cai W, Dai X, Chen J, Zhao J, Xu M, Zhang L, Yang B, Zhang W, Rocha M, Nakao T, Kofler J, Shi Y, Stetler RA, Hu X, Chen J (2019) STAT6/Arg1 promotes microglia/macrophage efferocytosis and inflammation resolution in stroke mice. JCI Insight 4:e131355.

Candelario-Jalil E, Dijkhuizen RM, Magnus T (2022) Neuroinflammation, stroke, blood-brain barrier dysfunction, and imaging modalities. Stroke 53:1473-1486.

Chen X, Dou J, Fu Z, Qiu Y, Zou L, Huang D, Tan X (2022) Macrophage M1 polarization mediated via the IL-6/STAT3 pathway contributes to apical periodontitis induced by Porphyromonas gingivalis. J Appl Oral Sci 30:e20220316.

Coles JA, Myburgh E, Brewer JM, McMenamin PG (2017) Where are we? The anatomy of the murine cortical meninges revisited for intravital imaging, immunology, and clearance of waste from the brain. Prog Neurobiol 156:107-148.

Császár E, et al. (2022) Microglia modulate blood flow, neurovascular coupling, and hypoperfusion via purinergic actions. J Exp Med 219:e20211071.

De Filippo K, Dudeck A, Hasenberg M, Nye E, van Rooijen N, Hartmann K, Gunzer M, Roers A, Hogg N (2013) Mast cell and macrophage chemokines CXCL1/CXCL2 control the early stage of neutrophil recruitment during tissue inflammation. Blood 121:4930-4937.

De Vlaminck K, Van Hove H, Kancheva D, Scheyltjens I, Pombo Antunes AR, Bastos J, Vara-Perez M, Ali L, Mampay M, Deneyer L, Miranda JF, Cai R, Bouwens L, De Bundel D, Caljon G, Stijlemans B, Massie A, Van Ginderachter JA, Vandenbroucke RE, Movahedi K (2022) Differential plasticity and fate of brain-resident and recruited macrophages during the onset and resolution of neuroinflammation. Immunity 55:2085-2102.e2089.

DeLong JH, Ohashi SN, O'Connor KC, Sansing LH (2022) Inflammatory responses after ischemic stroke. Semin Immunopathol 44:625-648.

Dhanesha N, Patel RB, Doddapattar P, Ghatge M, Flora GD, Jain M, Thedens D, Olalde H, Kumskova M, Leira EC, Chauhan AK (2022) PKM2 promotes neutrophil activation and cerebral thromboinflammation: therapeutic implications for ischemic stroke. Blood 139:1234-1245.

Drieu A, Lanquetin A, Levard D, Glavan M, Campos F, Quenault A, Lemarchand E, Naveau M, Pitel AL, Castillo J, Vivien D, Rubio M (2020) Alcohol exposure-induced neurovascular inflammatory priming impacts ischemic stroke and is linked with brain perivascular macrophages. JCI Insight 5:e129226.

Drieu A, Du S, Storck SE, Rustenhoven J, Papadopoulos Z, Dykstra T, Zhong F, Kim K, Blackburn S, Mamuladze T, Harari O, Karch CM, Bateman RJ, Perrin R, Farlow M, Chhatwal J, Hu S, Randolph GJ, Smirnov I, Kipnis J (2022) Parenchymal border macrophages regulate the flow dynamics of the cerebrospinal fluid. Nature 611:585-593.

Faraco G, Sugiyama Y, Lane D, Garcia-Bonilla L, Chang H, Santisteban MM, Racchumi G, Murphy M, Van Rooijen N, Anrather J, Iadecola C (2016) Perivascular macrophages mediate the neurovascular and cognitive dysfunction associated with hypertension. J Clin Invest 126:4674-4689.

Feigin VL, Brainin M, Norrving B, Martins S, Sacco RL, Hacke W, Fisher M, Pandian J, Lindsay P (2022) World Stroke Organization (WSO): Global stroke fact sheet 2022. Int J Stroke 17:18-29.

Garcia-Bonilla L, Shahanoor Z, Sciortino R, Nazarzoda O, Racchumi G, Iadecola C, Anrather J (2024) Analysis of brain and blood single-cell transcriptomics in acute and subacute phases after experimental stroke. Nat Immunol 25:357-370.

Gelderblom M, Leypoldt F, Steinbach K, Behrens D, Choe CU, Siler DA, Arumugam TV, Orthey E, Gerloff C, Tolosa E, Magnus T (2009) Temporal and spatial dynamics of cerebral immune cell accumulation in stroke. Stroke 40:1849-1857.

Goldmann T, et al. (2016) Origin, fate and dynamics of macrophages at central nervous system interfaces. Nat Immunol 17:797-805.

Han X, Li Q, Lan X, El-Mufti L, Ren H, Wang J (2019) Microglial depletion with clodronate liposomes increases proinflammatory cytokine levels, induces astrocyte activation, and damages blood vessel integrity. Mol Neurobiol 56:6184-6196.

Hao Y, Stuart T, Kowalski MH, Choudhary S, Hoffman P, Hartman A, Srivastava A, Molla G, Madad S, Fernandez-Granda C, Satija R (2024) Dictionary learning for integrative, multimodal and scalable single-cell analysis. Nat Biotechnol 42:293-304.

Hao Y, et al. (2021) Integrated analysis of multimodal single-cell data. Cell 184:3573-3587.e29.

Hawkes CA, McLaurin J (2009) Selective targeting of perivascular macrophages for clearance of beta-amyloid in cerebral amyloid angiopathy. Proc Natl Acad Sci U S A 106:1261-1266.

Hoffmann A, Miron VE (2024) CNS macrophage contributions to myelin health. Immunol Rev 327:53-70.

Hu C, Li T, Xu Y, Zhang X, Li F, Bai J, Chen J, Jiang W, Yang K, Ou Q, Li X, Wang P, Zhang Y (2023) CellMarker 2.0: an updated database of manually curated cell markers in human/mouse and web tools based on scRNA-seq data. Nucleic Acids Res 51:D870-D876.

Jin S, Guerrero-Juarez CF, Zhang L, Chang I, Ramos R, Kuan CH, Myung P, Plikus MV, Nie Q (2021) Inference and analysis of cell-cell communication using CellChat. Nat Commun 12:1088.

Jin W, Zhao J, Yang E, Wang Y, Wang Q, Wu Y, Tong F, Tan Y, Zhou J, Kang C (2022) Neuronal STAT3/HIF-1α/PTRF axis-mediated bioenergetic disturbance exacerbates cerebral ischemia-reperfusion injury via PLA2G4A. Theranostics 12:3196-3216.

Koneru R, Kobiler D, Lehrer S, Li J, van Rooijen N, Banerjee D, Glod J (2011) Macrophages play a key role in early blood brain barrier reformation after hypothermic brain injury. Neurosci Lett 501:148-151.

Li C, Xing Y, Zhang Y, Hua Y, Hu J, Bai Y (2022) Neutrophil extracellular traps exacerbate ischemic brain damage. Mol Neurobiol 59:643-656.

Liberzon A, Birger C, Thorvaldsdóttir H, Ghandi M, Mesirov JP, Tamayo P (2015) The Molecular Signatures Database (MSigDB) hallmark gene set collection. Cell Syst 1:417-425.

Liguz-Lecznar M, Zakrzewska R, Kossut M (2015) Inhibition of Tnf-α R1 signaling can rescue functional cortical plasticity impaired in early post-stroke period. Neurobiol Aging 36:2877-2884.

Lu Y, Shi M, Huang W, Li F, Liang H, Liu W, Huang T, Xu Z (2024) Diosmin alleviates NLRP3 inflammasome-dependent cellular pyroptosis after stroke through RSK2/CREB pathway. Brain Res 1848:149336.

Ma Y, Li Y, Jiang L, Wang L, Jiang Z, Wang Y, Zhang Z, Yang GY (2016) Macrophage depletion reduced brain injury following middle cerebral artery occlusion in mice. J Neuroinflammation 13:38.

Morabito S, Reese F, Rahimzadeh N, Miyoshi E, Swarup V (2023) hdWGCNA identifies co-expression networks in high-dimensional transcriptomics data. Cell Rep Methods 3:100498.

Mrdjen D, Pavlovic A, Hartmann FJ, Schreiner B, Utz SG, Leung BP, Lelios I, Heppner FL, Kipnis J, Merkler D, Greter M, Becher B (2018) High-dimensional single-cell mapping of central nervous system immune cells reveals distinct myeloid subsets in health, aging, and disease. Immunity 48:380-395.e386.

Obeng JA, Amoruso A, Camaschella GL, Sola D, Brunelleschi S, Fresu LG (2016) Modulation of human monocyte/macrophage activity by tocilizumab, abatacept and etanercept: An in vitro study. Eur J Pharmacol 780:33-37.

Park L, Uekawa K, Garcia-Bonilla L, Koizumi K, Murphy M, Pistik R, Younkin L, Younkin S, Zhou P, Carlson G, Anrather J, Iadecola C (2017) Brain perivascular macrophages initiate the neurovascular dysfunction of Alzheimer Aβ peptides. Circ Res 121:258-269.

Paul S, Candelario-Jalil E (2021) Emerging neuroprotective strategies for the treatment of ischemic stroke: An overview of clinical and preclinical studies. Exp Neurol 335:113518.

Pedragosa J, Salas-Perdomo A, Gallizioli M, Cugota R, Miró-Mur F, Briansó F, Justicia C, Pérez-Asensio F, Marquez-Kisinousky L, Urra X, Gieryng A, Kaminska B, Chamorro A, Planas AM (2018) CNS-border associated macrophages respond to acute ischemic stroke attracting granulocytes and promoting vascular leakage. Acta Neuropathol Commun 6:76.

Percie du Sert N, et al. (2020) The ARRIVE guidelines 2.0: Updated guidelines for reporting animal research. PLoS Biol 18:e3000410.

Prescott K, Münch AE, Brahms E, Weigel MK, Inoue K, Buckwalter MS, Liddelow SA, Peterson TC (2023) Blocking of microglia-astrocyte proinflammatory signaling is beneficial following stroke. Front Mol Neurosci 16:1305949.

Ren X, Gao X, Li Z, Ding Y, Xu A, Du L, Yang Y, Wang D, Wang Z, Shu S (2024) Electroacupuncture ameliorates neuroinflammation by inhibiting TRPV4 channel in ischemic stroke. CNS Neurosci Ther 30:e14618.

Schneider CA, Rasband WS, Eliceiri KW (2012) NIH Image to ImageJ: 25 years of image analysis. Nat Methods 9:671-675.

Soldatos A, Toro C, Hoffmann P, Romeo T, Deuitch N, Brofferio A, Aksentijevich I, Kastner DL, Ombrello AK (2023) TNF-blockade for primary stroke prevention in adenosine deaminase 2 deficiency: a case series. Neurol Neuroimmunol Neuroinflamm 10:e200073.

Tan L, Liang J, Wang X, Wang Y, Xiong T (2024) Dual roles of microglia in the pathological injury and repair of hemorrhagic cerebrovascular diseases. Regen Med Rep 1:93-105.

Tang H, Gamdzyk M, Huang L, Gao L, Lenahan C, Kang R, Tang J, Xia Y, Zhang JH (2020) Delayed recanalization after MCAO ameliorates ischemic stroke by inhibiting apoptosis via HGF/c-Met/STAT3/Bcl-2 pathway in rats. Exp Neurol 330:113359.

Uekawa K, Hattori Y, Ahn SJ, Seo J, Casey N, Anfray A, Zhou P, Luo W, Anrather J, Park L, Iadecola C (2023) Border-associated macrophages promote cerebral amyloid angiopathy and cognitive impairment through vascular oxidative stress. Res Sq doi: 10.21203/rs.3.rs-2719812/v1.

Wang X, Wang Q, Wang K, Ni Q, Li H, Su Z, Xu Y (2022) Is immune suppression involved in the ischemic stroke? A study based on computational biology. Front Aging Neurosci 14:830494.

Wang X, Chen J, Shen Y, Zhang H, Xu Y, Zhang J, Cheng L (2024) Baricitinib protects ICIs-related myocarditis by targeting JAK1/STAT3 to regulate macrophage polarization. Cytokine 179:156620.

Wang Y, Yuan T, Lyu T, Zhang L, Wang M, He Z, Wang Y, Li Z (2025) Mechanism of inflammatory response and therapeutic effects of stem cells in ischemic stroke: current evidence and future perspectives. Neural Regen Res 20:67-81.

Wicks EE, Ran KR, Kim JE, Xu R, Lee RP, Jackson CM (2022) The translational potential of microglia and monocyte-derived macrophages in ischemic stroke. Front Immunol 13:897022.

Ye XC, Hao Q, Ma WJ, Zhao QC, Wang WW, Yin HH, Zhang T, Wang M, Zan K, Yang XX, Zhang ZH, Shi HJ, Zu J, Raza HK, Zhang XL, Geng DQ, Hu JX, Cui GY (2020) Dectin-1/Syk signaling triggers neuroinflammation after ischemic stroke in mice. J Neuroinflammation 17:17.

Yu G, Wang LG, Han Y, He QY (2012) clusterProfiler: an R package for comparing biological themes among gene clusters. OMICS 16:284-287.

Zhang K, Wang Y, Chen S, Mao J, Jin Y, Ye H, Zhang Y, Liu X, Gong C, Cheng X, Huang X, Hoeft A, Chen Q, Li X, Fang X (2023a) TREM2(hi) resident macrophages protect the septic heart by maintaining cardiomyocyte homeostasis. Nat Metab 5:129-146.

Zhang W, Xu M, Chen F, Su Y, Yu M, Xing L, Chang Y, Yan T (2023b) Targeting the JAK2-STAT3 pathway to inhibit cGAS-STING activation improves neuronal senescence after ischemic stroke. Exp Neurol 368:114474.

Zhang Y, Zhang W, Liu T, Ma Z, Zhang W, Guan Y, Chen X (2024) Upregulation of circ0000381 attenuates microglial/macrophage pyroptosis after spinal cord injury. Neural Regen Res 19:1360-1366.

Zhang G, Yao Q, Long C, Yi P, Song J, Wu L, Wan W, Rao X, Lin Y, Wei G, Ying J, Hua F (2025) Infiltration by monocytes of the central nervous system and its role in multiple sclerosis: reflections on therapeutic strategies. Neural Regen Res 20:779-793.

Zheng K, Lin L, Jiang W, Chen L, Zhang X, Zhang Q, Ren Y, Hao J (2022) Single-cell RNA-seq reveals the transcriptional landscape in ischemic stroke. J Cereb Blood Flow Metab 42:56-73.

Zhong Y, Gu L, Ye Y, Zhu H, Pu B, Wang J, Li Y, Qiu S, Xiong X, Jian Z (2022) JAK2/STAT3 Axis Intermediates Microglia/Macrophage Polarization During Cerebral Ischemia/Reperfusion Injury. Neuroscience 496:119-128.

Zhu H, Jian Z, Zhong Y, Ye Y, Zhang Y, Hu X, Pu B, Gu L, Xiong X (2021) Janus kinase inhibition ameliorates ischemic stroke injury and neuroinflammation through reducing NLRP3 inflammasome activation via JAK2/STAT3 pathway inhibition. Front Immunol 12:714943.

P-Reviewers: Sun R, Cao F, Venkatesan R; C-Editor: Zhao M; S-Editors: Yu J, Li CH; L-Editors: Crow E, Yu J, Song LP; T-Editor: Jia Y

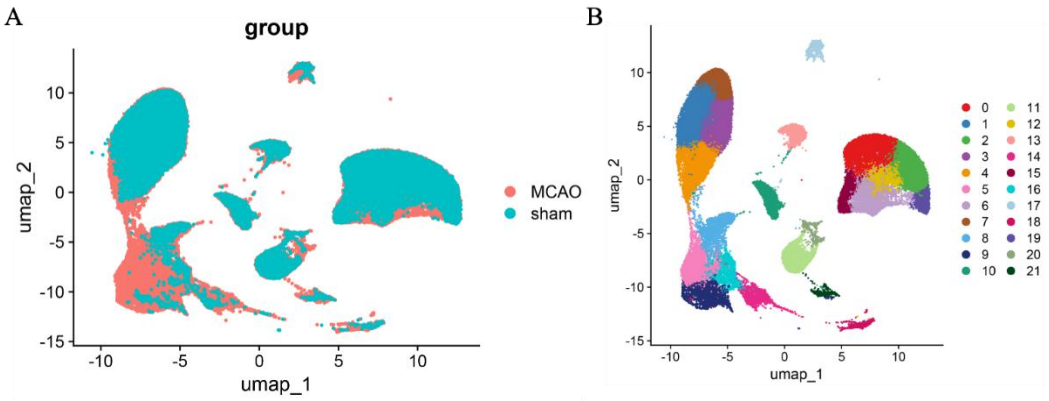

Additional Figure 1 The 74,826 cell annotations and clusters are visualized with UMAP.

(A) In the UMAP plots of the two groups, the cell clusters were completely merged, proving that the batch effect was eliminated; (B) all cells were divided into 22 clusters. UMAP: Uniform Manifold Approximation and Projection.

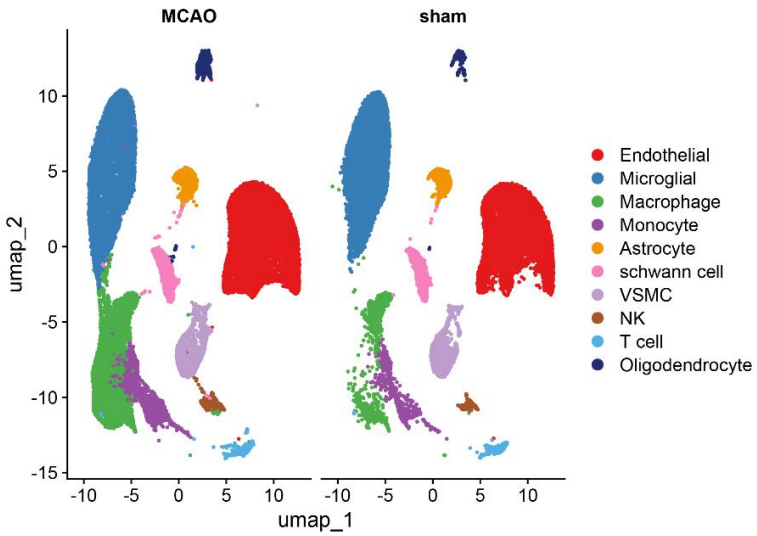

Additional Figure 2 The 74,826 cell type annotations divided by group.

The two groups of cells are identical. UMAP: Uniform Manifold Approximation and Projection.

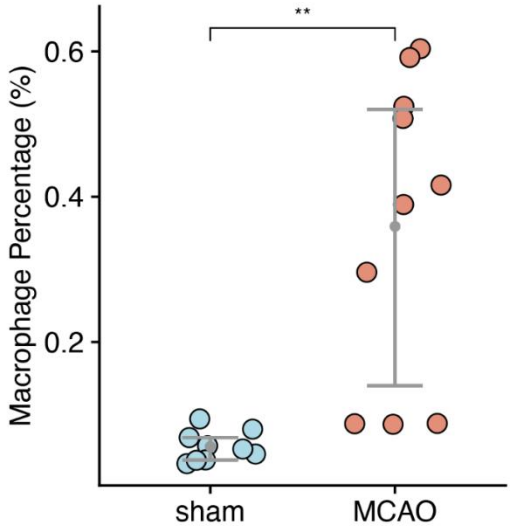

Additional Figure 3 The proportion of macrophages in the two groups.

Data are expressed as mean ± SD. $^{**}P < 0.01$ (two-tailed Student's t-test). MCAO: Middle cerebral artery occlusion.

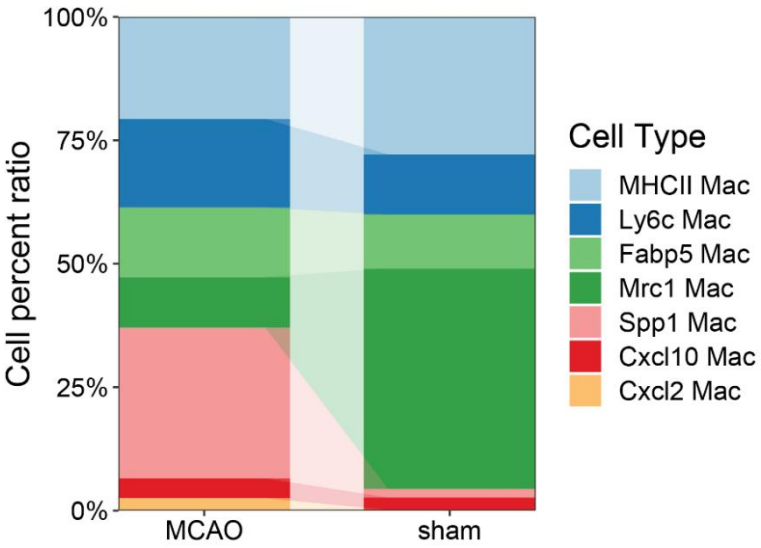

Additional Figure 4 The proportions of each macrophage cluster in the two groups.

MCAO: Middle cerebral artery occlusion.

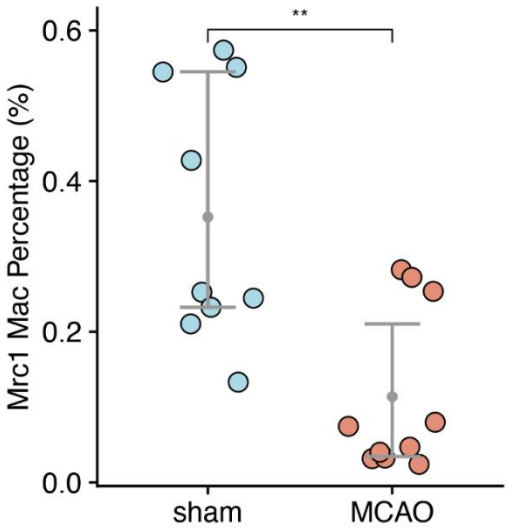

Additional Figure 5 The proportions of Mrc1 macrophage in the two groups.

Data are expressed as mean ± SD. $^{**}P < 0.01$ (two-tailed Student's t-test). MCAO: Middle cerebral artery occlusion.

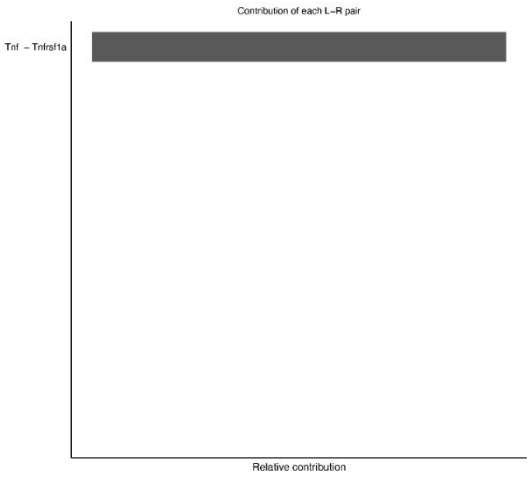

Additional Figure 6 Contributions of each ligand–receptor pair to the TNF pathway.

TNF: Tumor necrosis factor.

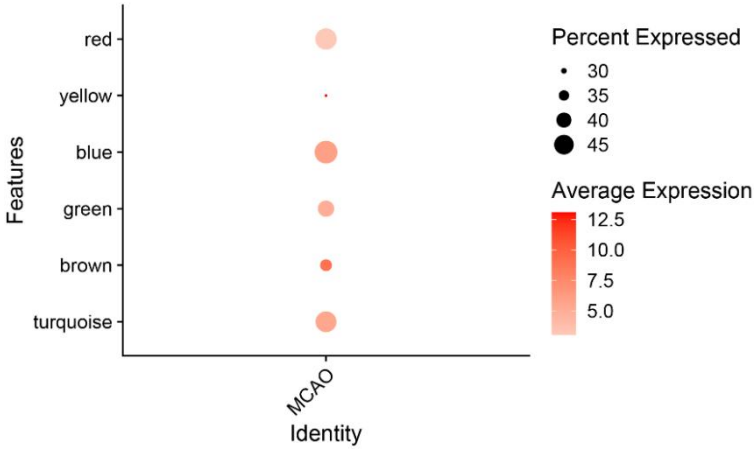

Additional Figure 7 The relationship between each module and ischemic stroke.

MCAO: Middle cerebral artery occlusion.

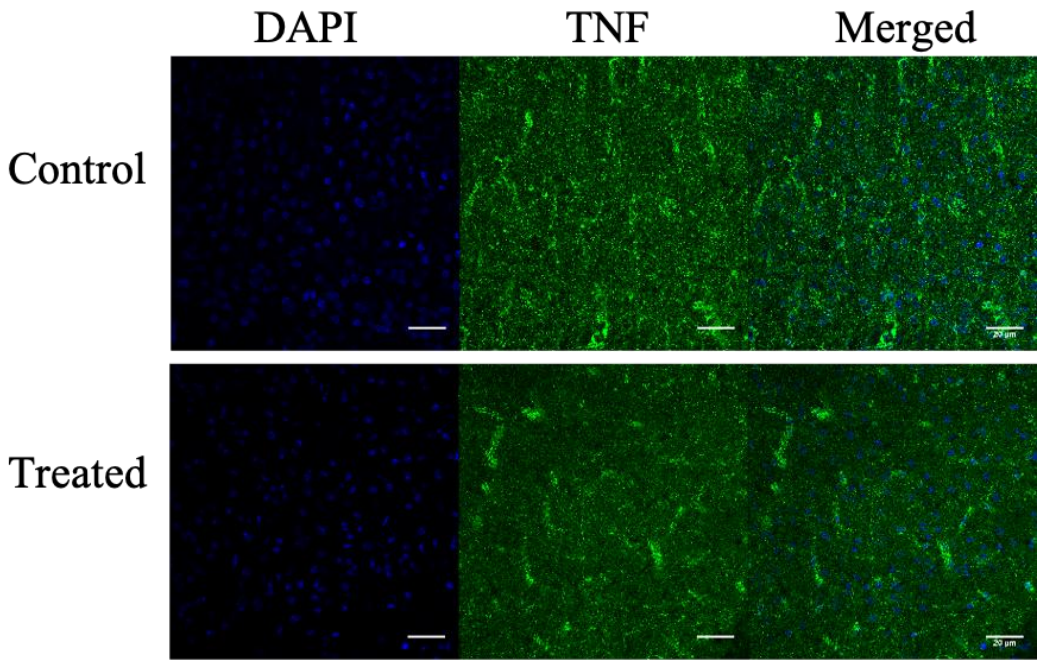

Additional Figure 8 Immunofluorescence staining for DAPI (blue) and TNF (green, stained by CL488) in the control and treated groups.

Compared with the control group, less TNF expression was observed in the treated group. Scale bars: 20 μm. DAPI: 4', 6-diaminidine-2-phenylindole; TNF: tumor necrosis factor.

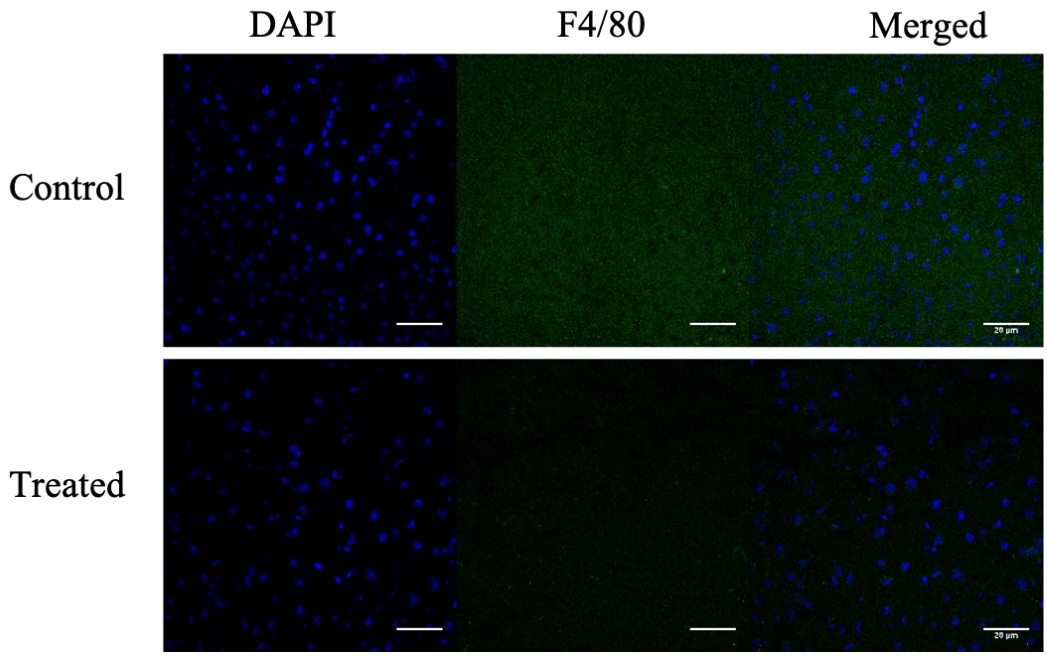

Additional Figure 9 Immunofluorescence staining for DAPI (blue) and F4/80 (green, stained by CL488) in the control and treated groups.

Compared with the control group, less F4/80 expression was observed in the treated group. Scale bars: 20 μm. DAPI: 4', 6-diaminidine- 2-phenylindole.

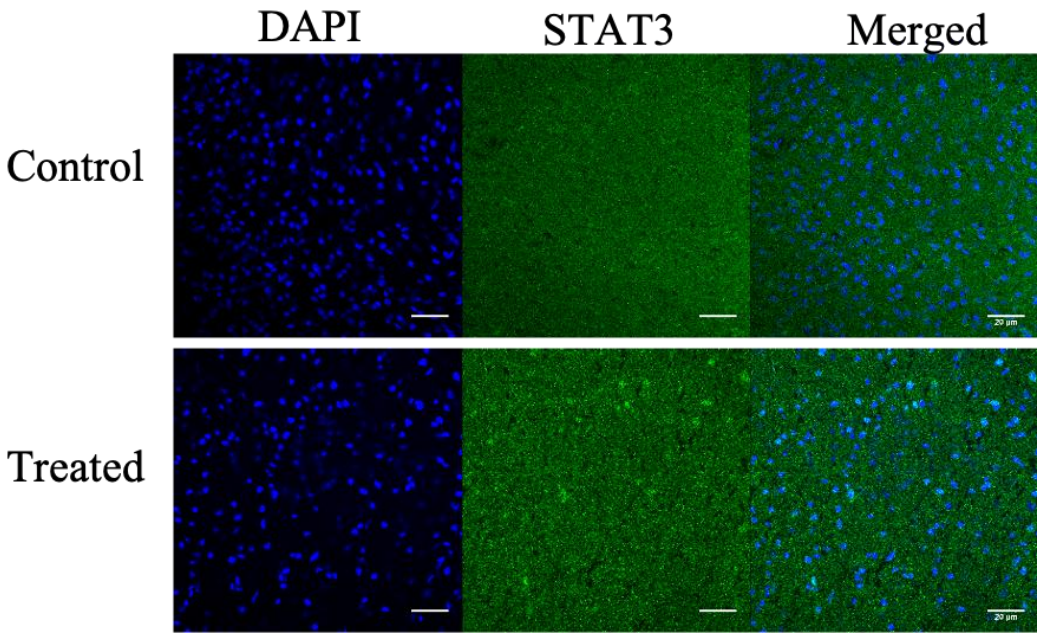

Additional Figure 10 Immunofluorescence staining for DAPI (blue) and STAT3 (green, stained by CL488) in the control and treated groups.

No significant difference was found in STAT3 expression between the two groups. Scale bars: 20 μm. DAPI: 4', 6-diaminidine-2-phenylindole; STAT3: signal transducer and activator of transcription 3.

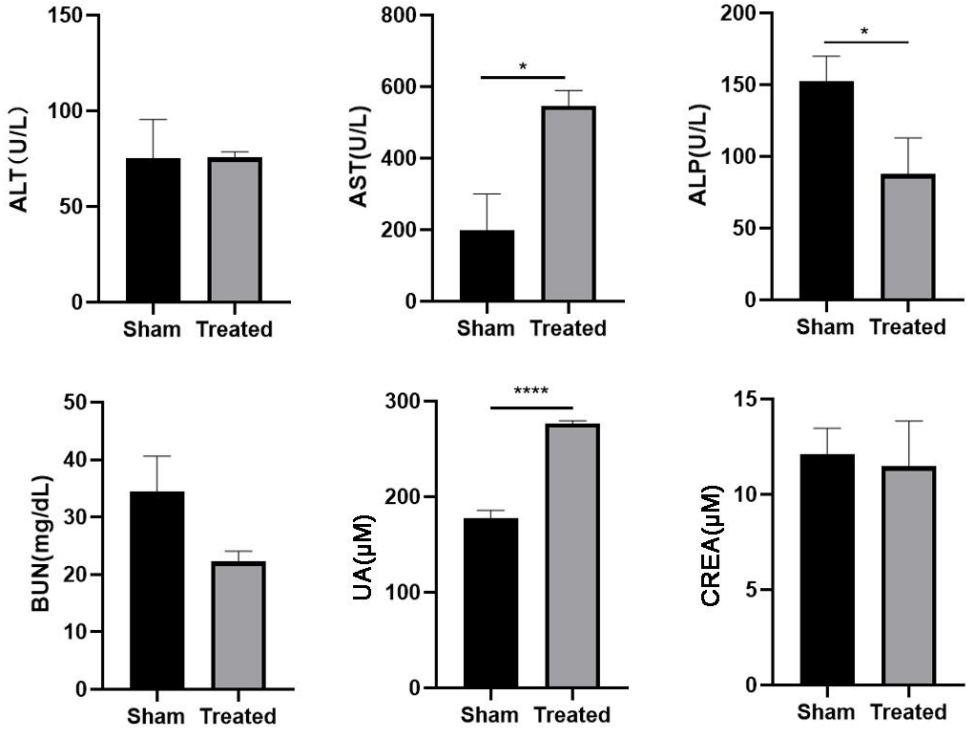

Additional Figure 11 Blood biochemical characterization of liver and kidney function.

Data are expressed as mean ± SD. *P < 0.05, ****P < 0.0001 (two-tailed Student's t-test). ALP: Alkaline phosphatase; ALT: alanine transaminase; AST: aspartate Aminotransferase; BUN: blood urea nitrogen; CREA: creatinine; UA: uric acid.

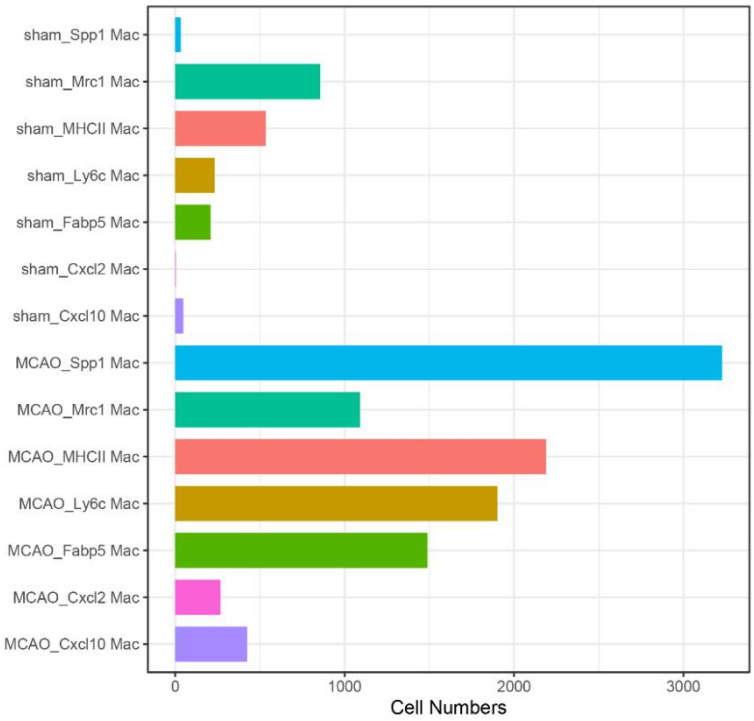

Additional Figure 12 The number of cells in each macrophage cluster in the sham and MCAO groups.

MCAO: Middle cerebral artery occlusion.

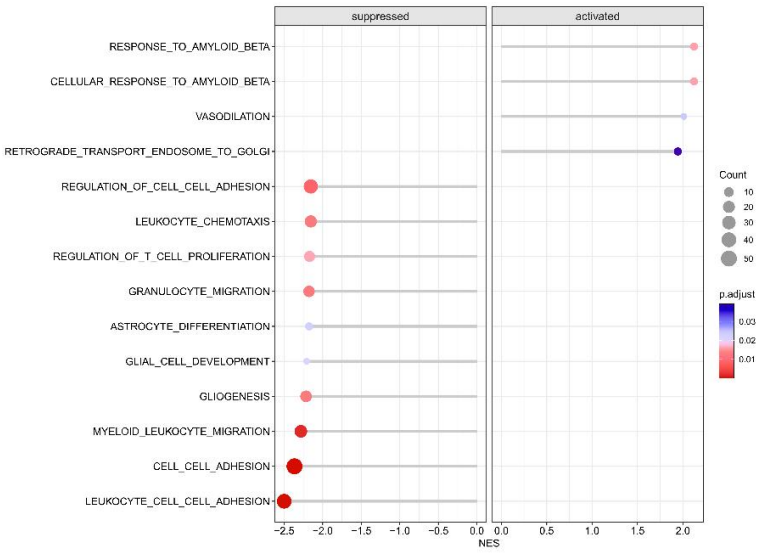

Additional Figure 13 The GSEA results show distinct BAM profiles in the acute and recovery phases of ischemic stroke.

Activated pathways were enriched in the recovery phase of ischemic stroke, while suppressed pathways were enriched in the acute phase. BAMs: border-associated macrophages; GSEA: Gene Set Enrichment Analysis.